

SIMULATION OF LARGE ICE MASS FLOW

by

JOHN VAN EGMOND, B. Eng. (CIVIL ENGINEERING)

A Thesis

Submitted to the School of Graduate Studies
in Partial Fulfilment of the Requirements
for the Degree
Master of Engineering

McMaster University

December, 1978

SIMULATION OF LARGE ICE

MASS FLOW

MASTER OF ENGINEERING (1978)
(Civil Engineering)

McMASTER UNIVERSITY
Hamilton, Ontario

TITLE: Simulation of Large Ice Mass Flow

AUTHOR: John Van Egmond, B. Eng., (McMaster University)

SUPERVISOR: Dr. John J. Emery

NUMBER OF PAGES: 108, ix

ABSTRACT

The finite element method has recently become a well-established technique in solving geotechnical problems, and has in the past few years been applied in glaciology to simulate ice mass flow problems. In fact, the models available have advanced much more rapidly than knowledge of the physical parameters and laws which describe ice needed in the simulation process. In this thesis, several functional flow laws are developed.

These laws, it is hoped, will lead to a better flow simulation for ice masses. Parameters such as grain size, age, and fabric, though poorly controlled in the testing of ice, are very important to the flow characteristics of ice as can be shown from a consideration of dislocation movements. A more systematic treatment of these parameters is needed.

The influence of initial stresses on flow behaviour not considered in previous finite element method simulations of glacier flow, is shown to be significant. Two finite element schemes are compared, and a scheme based on an implicit approach appears to be somewhat faster in computer time.

The importance of temperature to glacier flow is considered in this thesis. It is shown that non-isothermal conditions significantly affect the flow of ice masses.

The functional flow laws, and the non-isothermal temperature distribution are used to simulate flow of the Barnes Ice Cap. The simulation is found to be poor compared to observed results. It is felt that a consideration of initial stresses, better temperature distribution data, and improved flow laws are needed before the finite element method simulation will lead to satisfactory results.

ACKNOWLEDGEMENTS

In presenting this thesis, the author wishes to thank the following individuals:

- Debbie, his wife, for her support, encouragement, patience, and cheerfulness.
- Dr. J.J. Emery, his supervisor, for involving him in this work, for his patience and support.
- Dr. F. Mirza, for many hours of discussions, for his encouragement and his help.
- Dr. Y. Vaid, and Mr. E. Hanafy, for their helpful discussions.
- Environment Canada, Glaciology Division, for supporting him financially, and providing valuable field data for the Barnes Ice Cap.

Finally, this thesis is dedicated to his brother, Mark, who has taught him that to strive to become more than you are leads to success, and that to be what you are is success.

TABLE OF CONTENTS

		Page
CHAPTER 1	INTRODUCTION	1
1-1	Ice Mass Flow Simulation	1
1-2	Glaciers	2
1-2.1	Glacier Flow	2
1-2.2	Glacier Temperatures	5
1-3	Ice Formation, Density, Fabric and Impurities	5
1-3.1	Numerical Modelling	6
CHAPTER 2	FLOW RELATIONSHIP FOR ICE	8
2-1	Creep	8
2-2	Terminology and Method	9
2-2.1	Terminology	9
2-2.2	Methods	12
2-3	Review of Empirical Laws	14
2-4	Hooke's and Meier's Laws	26
2-4.1	Hooke's Law	26
2-4.2	Meier's Law	27
2-4.3	Functional Flow Relationship	28
2-4.3a	Functional Relationships H_{BTW} and H_W	28
2-4.3b	Functional Relationships M_1 and M_2	33
2-5	Flow Relationship for Ice Developed from Micro-mechanistic Consideration	36
2-6	Summary	40

CHAPTER 3	INFLUENCE OF INITIAL STRESSES	42
3-1	Initial Stresses	42
3-2	Stress States Assumed	44
3-3	Typical Ice Mass and Steady State Flow	48
3-4	Results	51
3-5	Surging	60
3-6	Discussion and Methods of Dealing with Initial Stresses	63
CHAPTER 4	TEMPERATURE INFLUENCES ON GLACIER FLOW	65
4-1	Temperature Influences	65
4-2	Ice Masses Considered	66
4-3	Flow Relationships Considered	70
4-4	Discussion of Results	71
4-5	Thermal Properties of Ice and Ice Masses	79
4-6	Summary	85
CHAPTER 5	CONCLUSION	87
5-1	Conclusion and Summary	87
REFERENCES		91
APPENDIX 1	SHEAR STRESS	97
APPENDIX 2	DISLOCATIONS, DEFECTS AND DEFORMATION	101

LIST OF FIGURES

FIGURE	TITLE	Page
1.1	Barnes Ice Cap	3
2.1	Temperature stress limits of research	23
2.2	Stress-strain rate limits	24
2.3	Various laws	29
2.4	Meier's Law at 0°C linearized	30
3.1	Stress states	45
3.2	Strain schemes	49
3.3	Ice mass studied	50
3.4	Equivalent stress	54
3.5	Cases 6-13 Equivalent stress	57
3.6	Cases 6-13 Horizontal stress	58
3.7	Equivalent stress - explicit scheme	60
3.8	Equivalent stress - implicit scheme	61
3.9	Comparison of steady state flow rates, Barnes Ice Cap	62
4.1	Barnes Ice Cap temperature distribution	67
4.2	12 Element mesh temperature distributions	68
4.3	48 Element mesh temperature and velocity distributions	69
4.4	Equivalent stress - Element 12 of 12 element mesh	72
4.5	Comparison of steady state flow rates from Barnes Ice Cap	76
A1.1	Glacier section	98
A2.1	Types of defects	102
A2.2	Crystal under stress	105

LIST OF TABLES

TABLE	TITLE	PAGE
2-1	Glacier homologous temperatures	13
2-2	Typical flow laws	16
2-3	Constants for laws in Table. 2-2a as proposed by various researchers	17-21
2-4	Range of parameters for various sets of results	22
2-5	Activation energy	32
2-6	Functional form M_2 from $\dot{\epsilon} = A(\sigma) \sigma^{n(\sigma)} e^{-AE/K_B T}$	35
2-7	Typical micro-deformation parameters for ice	38-39
3-1	Stress states and schemes used in simulation	52-53
3-2	Steady state surface flow rates	56
4-1	Equivalent stress as a function of time	73
4-2	Steady state surface velocities	74
4-3	Hypothetical summer surface velocities	78
4-4	Thermal conductivity of ice	81
4-5	Typical geothermal flux - northern Canada	83
4-6	Coefficient of thermal expansion	86
A2-1	B of Diffusion equation	104

CHAPTER 1

INTRODUCTION

1-1

ICE MASS FLOW SIMULATION

Using the incremental, initial strain, finite element method approach, a number of creep problems in soil and rock mechanics have been studied previously at McMaster University (1,2,3). Ice mass flow problems, that have generally been difficult to simulate using standard approximation methods, can also be examined using a similar finite element approach (4,5,6). Complex stress and temperature distributions, constitutive relationships, and boundary conditions can be dealt with efficiently using finite element method simulations. In this study, constitutive relationships for ice, initial stress influences on ice mass flow (normally considered small (7,8)), and the temperature distribution of ice masses have been considered, since these topics require detailed attention in the development of realistic simulation methods.

In Chapter Two, functional creep relationships are developed based on a survey of available empirical relationships, coupled with a consideration of the micro-mechanistic behaviour of ice. The influences of initial stress states and temperatures are then considered in Chapters Three and Four. Large deformations and

surging, which are of specific interest to the Barnes Ice Cap (Figure 1) are then also considered briefly in Chapter Three. Two finite element method formulations of the flow problem solution are also compared in Chapter Three (explicit and implicit approaches). A Summary of the work done and recommendations for future studies are given in the concluding Chapter.

Before turning to these more detailed aspects of the study, introductory material on glaciers, ice and numerical modelling approaches will be given. For detailed information on glaciers a number of excellent references are available (7,9, Journal of Glaciology).

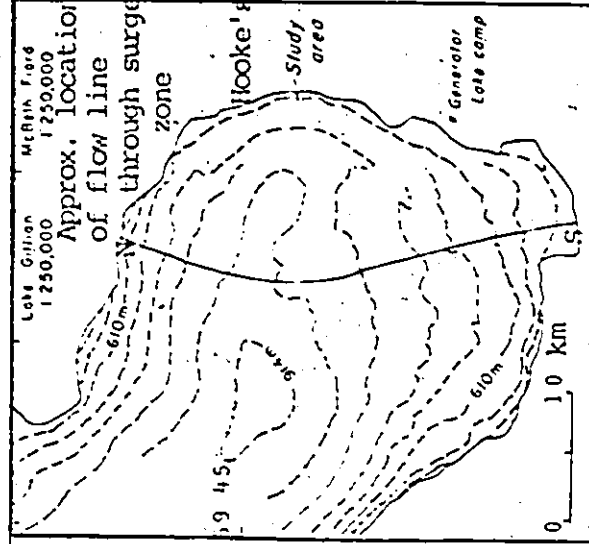
1-2

GLACIERS

Ice masses cover approximately 10% of the land surface of the earth, are responsible for many of our present landforms, are important to world weather systems, and may become crucial to the world's fresh water supply (7, 9). For these reasons alone, the dynamics of large ice masses is important. In this regard, the rapid advance of glaciers (surging) is of particular concern because it may be indicative of broad climactic changes. Potential large scale surging of the Antarctic ice mass, is particularly disturbing because it is estimated that such surging could cause the mean ocean level to rise by 30 meters, thus flooding many of the world's largest cities (9).

1-2.1 GLACIER FLOW

The movement of glaciers is well documented, and is due

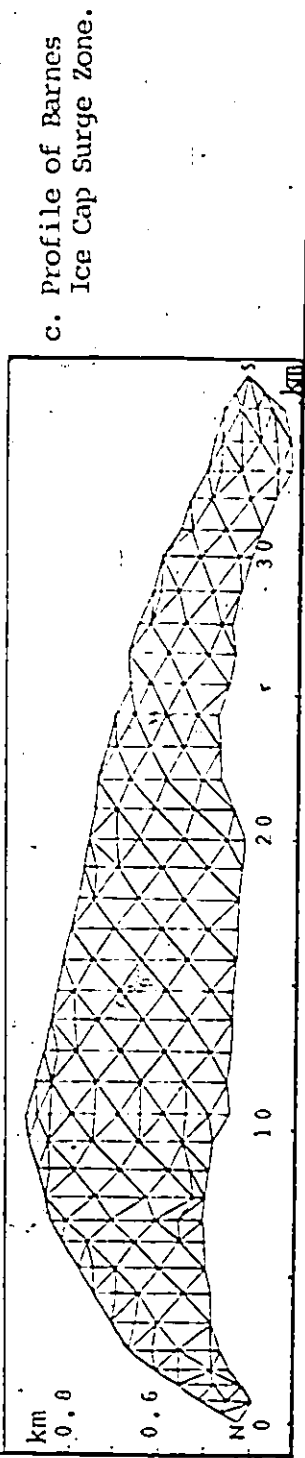


a. Barnes Ice Cap
Baffin Island
N.W.T. Canada.

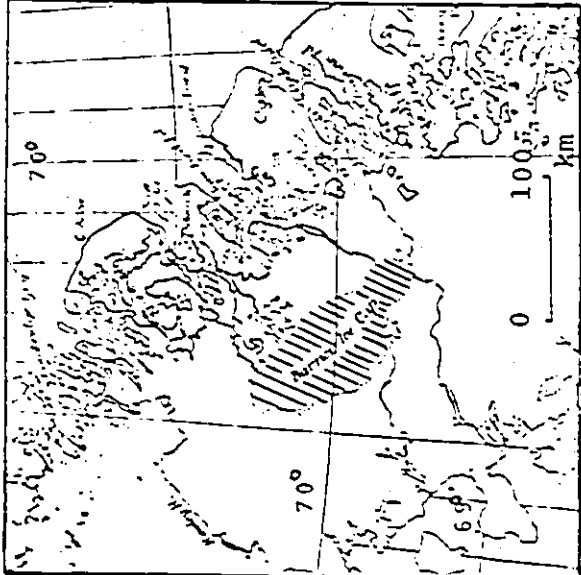
Taken from Hooke (15)

b. Region of Study

1. flow line known (-16)
2. Hooke (15)



c. Profile of Barnes
Ice Cap Surge Zone.



Taken from Mercer (14)

FIGURE 1-1 BARNES ICE CAP

to both basal sliding and internal deformation (creep). The motion of glaciers may be continuous, although short or long term velocity fluctuations are common (10,11).

BASAL SLIDING AND SURGING

Basal sliding (i.e. movement of the glacier as a rigid body over bedrock), although it is poorly understood, appears to involve both pressure melting at obstacles (regelation) and friction type sliding (slip) (11,12). Surging is the most dramatic case of basal sliding. Many stagnant, or slowly moving ice masses may suddenly (in glacial terms) advance at rates of several kilometers per year from average rates of several meters per year. The result of this surging is typically: emptying of the basin feeding the glacier; crevassing of the glacier surface; and thickening of the glacier terminus. Surging may be triggered by some or all of the following: accumulation leading to large loading; climactic changes leading to softening; basal heating (friction or heat from earth); or lubrication at the bed of the glacier.

CREEP

Glaciers also deform slowly by creep and this "steady state" aspect of ice mass dynamics has received the most attention. For instance, Nye has considered the velocity and stress distribution of glaciers, boundary effects, glacial cavities, ice falls, etc., assuming such continuous deformations occurred (13). The ice mass of most concern to this study is the Barnes Ice Cap, Baffin Island, Canada, (Figure 1), which is a remnant of the last ice age. Through

interaction with Environment Canada, Glaciology Division, data on surface velocities, surging, topography and temperature of the Barnes Ice Cap has been made available to this study. It is considered that this interaction with the Division will eventually allow a realistic simulation of the Barnes Ice Cap to be developed.

1-2.2 GLACIER TEMPERATURES

A glacier is classified according to its temperature distribution, which is a function of previous history, basal energy flux and surface temperature and other factors. A glacier at the pressure melting temperature throughout is termed temperate (also approximately 0°C). If glacier temperatures are below the pressure melting temperature, the glacier is termed cold. The world's two largest ice masses (Greenland and Antarctica) are predominantly cold (17) although basal layers may be at the pressure melting temperature (important in surging).

1-3 ICE FORMATION, DENSITY, FABRIC, AND IMPURITIES

Pure crystalline ice has a hexagonal arrangement of molecules (18) and a density of 0.917 g/cm^3 (19). Glacier ice forms slowly from snow due to a melting and refreezing process at grain boundaries under the influence of weight accumulation, melt water and temperature (17,20,21). Densification processes change the snow density from about 0.20 g/cm^3 to 0.92 g/cm^3 , subsequently influencing the flow of the ice (15,22). In most glacier ice, the C axis (vertical axis of the hexagonal crystals)

has become oriented in a predominant direction, and this fabric is detected as banding or foliation. Such fabric development has a significant influence on the response of ice and must be considered when constitutive relationships are developed. Most glacier ice contains very few impurities. However, the purity of glacier ice is still very important when dealing with any flow law for ice based on measurement of flow rates of natural and artificial ice masses, since it has been found that the presence of even a few parts per million of certain impurities can either harden or soften ice (15,23). Elastic properties of ice used in this study are Young's modulus (γ) of 8.34 to 9.1 $\times 10^3$ MPa, and Poisson's ratio (ν) of .34 to .35, based on typical values from the literature.

1-3.1 NUMERICAL MODELLING

Mathematical representation of problems, including boundary and initial conditions, can be done in a variety of ways. The most obvious is to seek an exact solution. However, this is usually not possible except for simple problems subject to rather restrictive boundary conditions. When an exact solution can not be found, finite difference or finite element methods can be used. Finite element discretization of engineering structures (dams, bays, etc) is a recent development since the method requires the computational effort only computers can provide. The finite element method can be used to solve complex problems and for the reader interested in more details, a number of references are available (1,24). In

this thesis two finite element formulations of creep flow problems have been used. The explicit scheme (2,3) calculates the solution at the next iteration as a function of the stress which is constant during the present iteration, while in the implicit solution, the solution calculated is a function of the changing stress. The implicit solution is a faster scheme.

These schemes have been used in conjunction with the various functional flow laws developed in the next chapter to simulate the flow of large ice masses.

CHAPTER 2
FLOW RELATIONSHIPS FOR ICE

2-1

CREEP

In common with many materials, ice exhibits permanent, time dependent deformations that are a function of the stress and temperature levels involved, assuming the deformations are not introducing gross material changes (i.e. constant fabric) (25,26). This flow (creep) behaviour is generally considered to be thermally activated, and in fact, glacier ice is responding as a material at high temperatures, since its homologous temperature T_H (ratio of material temperature to melting temperature) approaches unity for typical glacier temperatures of -20°C to 0°C (27,28, 29). While only the flow of large ice masses such as glaciers is considered here, there are many other areas where a knowledge of ice creep is required. Examples would include: service tunnels in ice; deep drilling through glaciers during oil exploration and development; military and scientific stations within large ice masses; iceberg development at ice margins; and mining of ore bodies under glaciers (20, 22,30). Obviously, any new developments in the simulation of glacier flow will be of

benefit to these other areas of ice mechanics, and the general area of geotechnology.

The flow behaviour of ice has been studied by many researchers, and a synthesis of this work is given in following sections. The ultimate acceptability and usefulness of any ice flow relationship developed will depend on how representative the ice tested is of the actual ice in the glacier being considered. However, some terminology used throughout the rest of this study, and the methods adopted by researchers in the past, is discussed before considering the applicability of available flow relationships and the laboratory and/or field data used during their development.

2-2

TERMINOLOGY AND METHODS

2-2.1 TERMINOLOGY

While most experimental or field based flow relationships are uniaxial in nature, actual creep problems are multiaxial, both in stress and strain states, and to summarize the extensive previous research, the concept of an equivalent stress* and equivalent strain rate from classical plasticity and creep analysis is adopted. Many possible definitions of effective stress

*The term "effective" is used in the metallurgy literature. However, to avoid confusion with geotechnology concepts, the term "equivalent" is adopted in this study.

have been given, however, one that preserves the uniaxial form is adopted here (Dorn's definition):

$$\sigma_D = \left(\frac{1}{2} \left((\sigma_x - \sigma_y)^2 + (\sigma_y - \sigma_x)^2 + (\sigma_z - \sigma_x)^2 + 6\tau_{xy}^2 \right) \right)^{1/2} \quad (2-1a)$$

$$= 3/\sqrt{2} \tau_{oct} \quad (2-1b)$$

where σ_D is the equivalent stress, σ_x , σ_y , and σ_z are the normal stresses in the x, y, and z directions, τ_{xy} is the shear stress in the xy plane, and τ_{oct} is the octahedral shear stress. Since Dorn's definition actually gives the equivalent stress in terms of stress invariants, the equivalent stress is obviously of constant magnitude regardless of axes orientation. It should be noted that Equation 2-1a is applicable for the plane strain case.

It has been shown in plasticity theory that the incremental strains are related to the stresses (2,32,26,31). Flow laws for this reason are generally defined in terms of strain rates rather than total strains.

The equivalent strain rate adopted here, that again preserves the uniaxial form, is Dorn's definition which is obtained as the time derivative of the equivalent strain. This equivalent strain ϵ_D is given by:

$$\epsilon_D = \left(2 \left((\epsilon_x - \epsilon_y)^2 + \epsilon_y^2 + \epsilon_x^2 + 6\epsilon_{xy}^2 \right) \right)^{1/2} / 3 \quad (2-2a)$$

$$= 2/\sqrt{3} \epsilon_{oct} \quad (2-2b)$$

where ϵ_x and ϵ_y are the strain in the x and y directions, ϵ_{xy} is the shear strain, and ϵ_{oct} the octahedral strain. Equation 2-2a is again for the plane strain case.

Another specific stress commonly encountered in glaciology is the basal shear stress due to the downhill component of an ice mass on a simple slope. This is given by (see derivation in Appendix 1):

$$\tau = \rho g h a_s \quad (2-3)$$

where τ is the shear stress, ρ is the ice density, h is the depth of ice, g is the acceleration due to gravity, and a_s is the surface slope of the ice mass. Implicit in this expression is the assumption that the basal and surface slopes of the ice mass are approximately equal.

Because it may seem strange to consider the flow of ice a high temperature phenomenon, it is worthwhile to define the homologous temperature (27,28,29):

$$T_H = T_M / T_{\text{melt}} \quad (2-4)$$

where T_H is the homologous temperature, T_M is the material temperature, and T_{melt} is the melting temperature of the material. Further, if the normalized stress σ_n is defined as:

$$\sigma_n = \sigma / G \quad (2-5)$$

where σ is the stress level and G is the shear modulus, it is found that groups of materials at comparable homologous temperature and normalized stress behave in a similar manner and have the same dominant micro-mechanisms acting (27, 28,29). From the definition of homologous temperature, and the

data in Table 2-1, it can be seen that ice, as it normally exists, is certainly a material at high temperature ($T_H > 0.78$).

2-2.2 METHODS

Flow laws for ice have been derived from either laboratory or field measurements of known stresses and/or strain rates, and are typically put in some form of uniaxial flow relationship. To extend these relationships to the more applicable in situ multiaxial flow case, the equivalent stress and strain rate are used to replace uniaxial terms. Further, the components of strain rate are then generally found by applying the Prandtl-Reuss assumptions from plastic flow theory as indicated in Nye's work (33).* It is also possible to develop flow laws for ice if the strain rate components and the stresses are known.

Laboratory results are most often obtained using uniaxial testing methods (34, 35, 36), although beam bending (37, 38, 39, 40), shear tests (41), and indenter techniques (42) are also used. The state of stress is known more accurately during laboratory testing than in the field where many unknowns exist. However, it is difficult to ensure that the ice and testing conditions in the laboratory are representative of the in situ case.

* $\dot{\epsilon}_x = \lambda \sigma_x'$, $\dot{\epsilon}_{xy} = \lambda \tau_{xy}$ where $\sigma_x' = (\sigma_x + \sigma_y + \sigma_z)/3$
 $\lambda = A \tau^n$ where $\tau = \sqrt{3} \sigma_D$

TABLE 2-1
 Glacier Homologous Temperatures

T_h	Depth (meters)	Ref.	Location
0.780-0.982	0 < depth < base	17	Antarctica
0.911	> 10	20	Greenland, Neve
0.965-0.986	9.0 < depth < 61.0	30	Tuto
0.9998-1.00	500.	43	Athabaska
0.9994-0.9996	200.	43	Athabaska
0.9707	----	44	Tuto
0.999	18.5 < depth < 52.0	45	Taku, Alaska, ice and firn
0.938	00.0 < depth < 18.5	45	Taku, Alaska, firn
0.912-0.907	10.0 < depth < 410.	46	Greenland
0.896-0.897	10.0 < depth < 300.	46	Bryd Station
0.963-0.996	00.0 < depth < base	47	Barnes Ice Cap

Field measurements of the strain components, depth, temperature, and time taken over grids using surveying techniques, or boreholes using inclinometers, have also been used to establish flow relationships for ice (8,12,16, 20, 15,48,45,49). For instance, assuming that the temperature over the entire glacier is constant, and that the ice-rock interface remains intact, it is possible to determine a flow law from equations of surface velocity, equilibrium, and strain components. Obviously, such field monitoring is both expensive and time consuming, particularly when the remote location of ice masses such as the Barnes Ice Cap is considered. Often the monitoring will only cover a portion of the ice mass, and this must be considered along with the quality of the field data when evaluating flow relationships.

2-3

REVIEW OF EMPIRICAL LAWS

In the past, glacier ice was considered to behave as a Newtonian viscous fluid (7). In the early 1950's however, it was generally established that glacier ice behaves as a "plastic substance" following a power flow law. Since that time, many experimental and theoretical studies have been initiated to establish the appropriate flow law(s), and have been summarized in varying degrees of detail by various researchers (18,50). The general

forms of the main flow laws that have been proposed are given in Table 2-2. The flow law given by Equations 1 and 2 in Table 2-2 is the most common form found in the literature, probably because of its simplicity and ease of application. However, A and n have been given many different values by various researchers as can be seen in Table 2-3.

This raises the major problem of deciding which, if any, of the constants are best for a given problem, and requires a consideration of the in situ stresses, temperatures, and ice fabrics. The flow laws and constants describing them, as proposed by various researchers, are given in Table 2-3 where all constants have been made consistent with stresses in bars (1 bar = 0.1 MPa) and strain rates in year⁻¹ (a⁻¹), as these units are most often adopted in the glaciological literature.

The range of stresses, temperatures, densities, ages, grain sizes, fabrics, ice types, and test conditions for which various flow relationships have been developed are given in Table 2-4. Much of this information is summarized in Figure 2-1 and 2-2 with the limits of research to date for representative sets of data clearly indicated. The general areas applicable to the Barnes Ice Cap are also given in these figures.

From Table 2-4, it can be seen that if the grain

TABLE 2-2

TYPICAL FLOW LAWS*

Equation Number	Law	Comment
1	$\dot{\epsilon} = A \sigma^n$	single deformation mechanism
2	$\dot{\gamma} = A_1 \tau^n$ or $(\tau/\Lambda)^n$	single deformation mechanism
3	$\dot{\gamma} = A_1 \tau^n + A_2 \tau^n$	two simultaneous mechanisms
4	$\dot{\gamma} = A_1 \sinh(\tau/\tau_0)^n$	symmetric energy barrier
5	$\dot{\gamma} = A \sigma^n e^{-\Delta E/K_b T}$	rate process theory (Arrhenius)
6	$\dot{\gamma} = A (\sinh \alpha \sigma)^n e^{-\Delta E/K_b T}$	
7	$\dot{\gamma} = A e^{-\Delta E/K_b T} \sigma^{n+f(\sigma, T)}$	
8	$\dot{\gamma} = 2(\tau/\Lambda)^n / (T-273.16)$	
9	$\dot{\epsilon} = A \sigma/d^n$	diffusion deformation mechanism

* Λ, n, A_1, A_2 of the equations are not the same.

σ and τ are stresses (axial and shear), n is an exponent, Λ, A_1, A_2 are constants, ΔE is the activation energy, K_b is the Boltzmann constant, τ_0 is a constant, d is the grain size, ϵ and $\dot{\gamma}$ are the strain rates (axial and shear).

TABLE 2-3
 CONSTANTS FOR LAWS IN TABLE 2-2 AS PROPOSED BY VARIOUS RESEARCHERS
 (for stress in bars and strain rate in year⁻¹)

Researcher	A	n	*σ _D	*γ̇ _D	Comments
Hooke (15)	2.80	1.65	√3	2/√3	white, low density, in $\dot{\gamma} = (\tau/A)^n$
Hooke (15)	5.0	1.65	√3	2/√3	blue, coarse ice, in $\dot{\gamma} = (\tau/A)^n$
Hooke (15)	4.5	1.65	√3	2/√3	blue, fine ice, in $\dot{\gamma} = (\tau/A)^n$
Holdsworth, Bull (48)	0.63	1.9	√3	2/√3	stress 0.15 to 0.65 bars, $(\tau/A)^n$
Holdsworth, Bull (48)	---	4.5	√3	2/√3	stress 0.65 bars in $\dot{\gamma} = (\tau/A)^n$
Holdsworth, Bull (48)	6.44	1.6	√3	2/√3	based on hole closure, $\dot{\gamma} = (\tau/A)^n$
Holdsworth, Bull (48)	---	4.3	√3	2/√3	based on hole closure, $\dot{\gamma} = (\tau/A)^n$
Miller (45)	56.2	4.0	√3	√3	1951, equation 1
Miller (45)	0.7	3.0	√3	√3	1952, equation 1
Glen (35)	0.017	4.2	1	1	equation 1
Butkovich, Landauer (41,51)	0.296	2.96	√3	1/√3	
Holdsworth (16)	0.51	4.2	√3	2/√3	$\dot{\gamma} = (\tau/A)^n$

* to convert to Dorn's definition multiply by this factor

cont'd.....

TABLE 2-3 (Continued)
 CONSTANTS FOR LAWS IN TABLE 2-2 AS PROPOSED BY VARIOUS RESEARCHERS
 (for stress in bars and strain rate in year⁻¹)

EQUATION 1 or 2						
Researcher	Λ	$\langle n$	σ_D^*	$\dot{\gamma}_D^*$	Comments	
Hansen, Landauer (52)	---	3.77	--	--	used $\sigma = \rho gh$	
Nye (53)	0.175	3.07	$\sqrt{3}$	$2/\sqrt{3}$	in $\dot{\gamma} = (\tau/\Lambda)^n$	
EQUATION 3						
Researcher	Λ_1	Λ_2	n	σ_D^*	$\dot{\gamma}_D^*$	Comment
Meier (12)	0.018	0.13	4.5	$3/\sqrt{2}$	$\sqrt{2}$	field and laboratory
Mellor, Smith (22)	0.056	0.0047	3.5	$\sqrt{3}$	$2/\sqrt{3}$	-4°C, low density
Mellor, Smith (22)	0.047	0.0025	3.5	$\sqrt{3}$	$2/\sqrt{3}$	-4°C, low density
Butkovich, Landauer (41, 51)	0.129	0.284	3.0	$\sqrt{3}$	$1/\sqrt{3}$	

* to convert to Dorn's definition multiply by this factor

cont'd.....

TABLE 2-3 (Continued)
 CONSTANTS FOR LAWS IN TABLE 2-2 AS PROPOSED BY VARIOUS RESEARCHERS
 (for stress in bars and strain rate in year⁻¹)

EQUATION 4						
Researcher	A	τ_0	σ_D^*	$\dot{\gamma}_D^*$	Comments	
Mellor, Smith (22)	---	--	$\sqrt{3}$	2//3		
Butkovich, Landauer (41, 51)	0.334	1.1	$\sqrt{3}$	1//3		
EQUATION 5						
Researcher	A	n	ΔE , kcal/mole	σ_D^*	$\dot{\gamma}_D^*$	Comments
Mellor, Smith (22)	---	---	10.0	$\sqrt{3}$	2//3	
Glen (35)	---	4.2	32.0	1	1	ΔE high
Hudd (54)	---	---	1/10 to 1/11	-	-	use $e^{-\Delta E/T}$
Glen, Jones (23)	---	2.6	9.43	1	1	-50°C to -90°C
Glen, Jones (23)	---	2.6	15.46	1	1	-10°C to -50°C

cont'd.....

* to convert to Dorn's definition multiply by this factor

TABLE 2-3 (Continued)
 CONSTANTS FOR LAWS IN TABLE 2-2 AS PROPOSED BY VARIOUS RESEARCHERS

(for stress in bars and strain rate in year⁻¹)

EQUATION 5						
Researcher	A	n	ΔE kcal/mole	σ_D^*	γ_D^*	Comments
Higasaki (55)	---	1.58	15.8	1	1	basal glide (-40°C to -18°C)
Higasaki (55)	---	6.5	15.8	1	1	non basal glide
Barnes, Tabor, Walker (42)	7.65×10^{27}	3.14	28.97	1	1	-2°C to 8°C
Barnes, Tabor, Walker (42)	2.098×10^{19}	3.01	18.76	1	1	-8°C to -14°C
Barnes, Tabor, Walker (42)	2.276×10^{19}	2.98	18.81	1	1	-14°C to -22°C
Barnes, Tabor, Walker (42)	9.14×10^{18}	3.11	18.23	1	1	-22°C to -34°C
Barnes, Tabor, Walker (42)	10.64×10^8	3.18	16.06	1	1	-34°C to -45°C

*to convert to Dorn's definition multiply by this factor

cont'd.....

TABLE 2-3² (Continued)
 CONSTANTS FOR LAWS IN TABLE 2-2 AS PROPOSED BY VARIOUS RESEARCHERS

(for stress in bars and strain rate in year ⁻¹)									
EQUATION 6									
Researcher	A	n	$\frac{kcal}{\Delta E \text{ mole}}$	* σ_D	* $\dot{\gamma}_D$	Comments			
Barnes, Tabor, Walker (42)	1.45×10^{26}	0.0279	28.64	1	1	-2° to -8°C			
Barnes, Tabor, Walker (42)	9.90×10^{17}	0.0254	18.64	1	1	-8° to -14°C			
Barnes, Tabor, Walker (42)	5.93×10^{17}	0.0282	18.64	1	1	-8° to -22°C			
EQUATION 8									
Researcher	A	n	* σ_D	* $\dot{\gamma}_D$	Comments				
Shumskii (56)	3.1	3.0	$\sqrt{3}$	$2/\sqrt{3}$					
EQUATION 9									
Researcher	A	n	* σ_D	* $\dot{\gamma}_D$	Comments				
Bromer, Kingery (57)	---	1.95	1	1	at -9.9°C				

* to convert to Dorn's definition multiply by this factor

TABLE 2-4

RANGE OF PARAMETERS FOR VARIOUS SETS OF RESULTS*

Refer- ence	Density (g/cm ³)	Stress (bars)	C temperature	Age (weeks)	Size (mm)	Grain	Equation		Type of test
							Fabric	Ice Type of	
Glen (35)	0.917	1-10	0-(-12.5)	?	?	1.0	r	1,5	a L
Jellenik, Brill (58)	0.886	0.65-2.4	-5	0-10	0-10	1.0-2.0	r	1	a L
Jellenik, Brill (58)	0.917	0.65-2.4	-5	0-old	0-old	1x10	p	1	n,as L
Barnes, Tabor, Walker (42)	0.910	1.0-10.5	0-(-48.0)	?	?	1-2.0	r	6	a L
Steinman (36)	?	0.6-18.0	0-(-22.0)	?	?	0.85	r	7	a L
Butkovich, Landauer (51)	0.9-0.917	0.02-12.	-5	?-old	?-old	10-20	r,p	2,3,4	a,s L
Butkovich, Landauer (51)	0.9-0.917	0.02-12.	-5	?-old	?-old	3,5	p	2,3,4	n L
Meier (12)	0.85-0.91	0.0-1.0	0	old	old	1-100	r	3	n F
Holdsworth (16)	0.88-0.92	0.1-7.0	-18.0	old	old	1-4	p	2	n F
Hooke (15)	0.80-0.92	0.4 <	-10°	old	old	?	p	2	n F
Mellor, Smith (22)	0.4-0.83	0.1-20.0	-5-(-34.5)	>3	>3	0.1-0.85	r	3	a L

*Fabric: preferred orientation or random orientation.
 Type of Ice: artificial, natural, or single crystal.
 Type of Test: Field or Laboratory.
 Equations: Table 2-2.

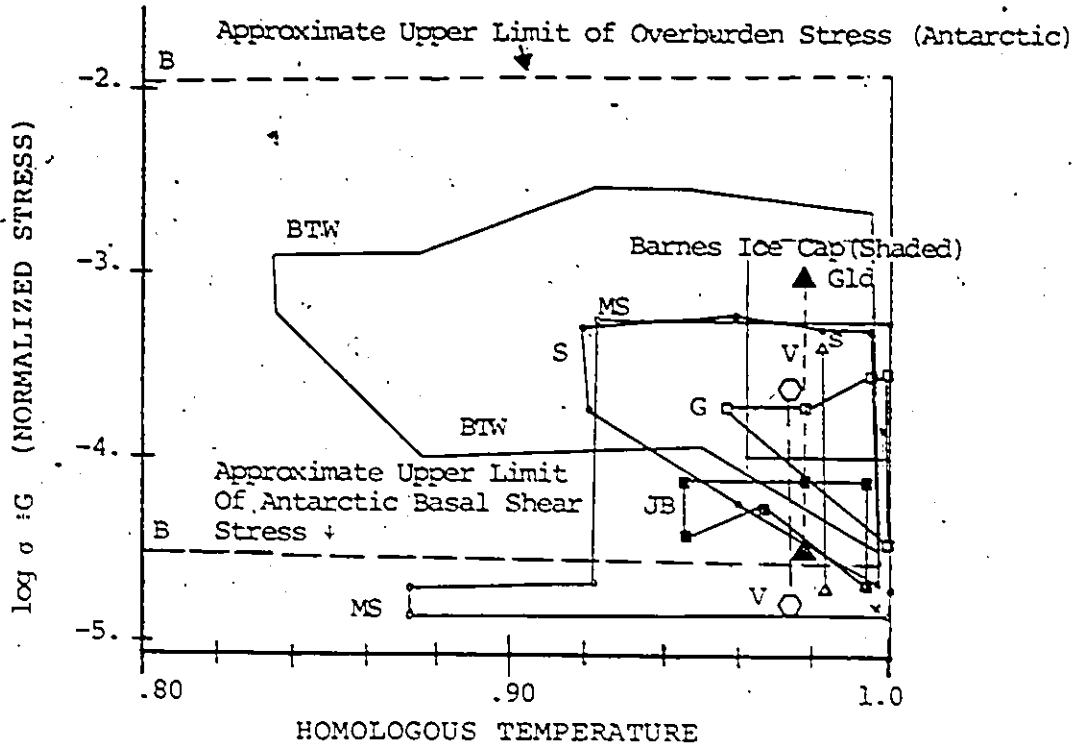
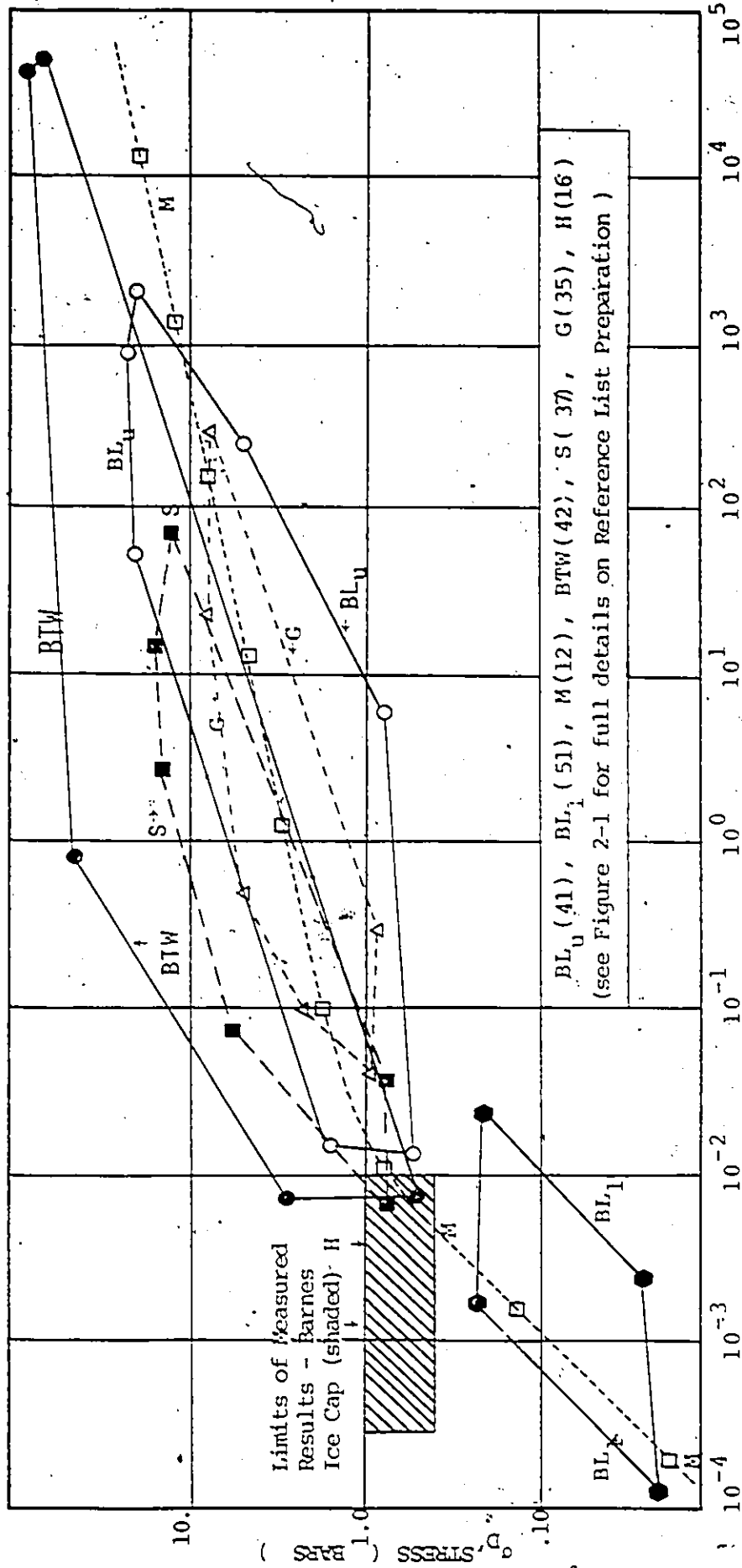


FIGURE 2-1 TEMPERATURE AND STRESS LIMITS OF RESEARCH

Reference List:

- BTW-Barnes, Tabor, Walker (42), oMS-Mellor, Smith (22),
- S-Steinman (36), Δ BL-Butkovich, Landauer (41),
- CV-Vialov (59), ■ JB-Jellenik, Brill (58); × R-Rigsby (60),
- CG-Glen (35), ▲ Gld-Gold (61), ---B-Budd, Jensen, Radok
- (17), Barnes Ice Cap (approximate limits of observed results (16)).



BL_U (41), BL₁ (51), M(12), BTW(42), S(37), G(35), H(16)
 (see Figure 2-1 for full details on Reference List Preparation)

$\dot{\epsilon}_D$, strain rate (yr⁻¹)

FIGURE 2-2 STRESS-STRAIN RATE LIMITS

size is an important factor governing the flow of glacier ice, then considerable variation in flow rates could exist over the stress-temperature range of interest due to this parameter's influence. In the past, experimentally derived laws for ice have primarily considered the influence of stress and temperature, although the influence of secondary factors such as repeated loading have also been considered (34,38). Laboratory and field studies of glacier ice fabric continue to be an important area of more recent research in glaciology that should yield the necessary information for eventually incorporating fabric influences into simulation approaches. Aspects such as grain size, air inclusions, age, etc. (i.e. key ice type parameters) must receive closer attention in future research.

Barnes, Tabor, and Walker (42) have suggested that the deformation of ice can be divided into three regions on the basis of temperature ranges. In each region a different micro-mechanism is acting. The fact that several mechanisms are contributing simultaneously to creep is a concept discussed in following sections with regard to the deformation mechanism space concept of Ashby, Frost, and Goodman(62).

In this study, two empirical flow laws from Table 2-3 - Meier's and Hooke's - have been used as base relationships from which functional flow laws that include temperature influences were developed. These laws are considered to be generally representative of the in situ condition of

typical large ice masses such as the Barnes Ice Cap. It should be noted that the development used, and the simulation programs, are not limited to these two laws. The flexibility exists in the programs to incorporate other features such as fabric, when adequate research results become available.

2-4 HOOKE'S AND MEIER'S LAWS

2-4.1 HOOKE'S LAW

Hooke used field measurements to determine the various constants for the flow law:

$$\dot{\epsilon} = (\tau/A)^{1.65} \quad (2-6)$$

where $\dot{\epsilon}$ is the strain rate, τ is the stress, and A is a constant (see Table 2-3). Much of Hooke's data was derived within 150 meters of the south dome margin of the Barnes Ice Cap from four boreholes and tunnels (see Figure 1-1). These field measurements gave close agreement to laboratory and independently derived field results. The ice showed fabric due to c-axis orientation (Page 4 of Chapter 1), and foliation due to the elongation of entrapped air bubbles, supporting the observation that the ice at the glacier margin was not homogeneous or isotropic. Hooke found that the Barnes Ice Cap could be divided into white (air entrained), coarse blue, and fine

blue ices, and that the ice often contained a fine silt not thought to influence its properties. Clearly, with all of these factors involved, the "field" ice should yield more realistic flow data than ice tested in the laboratory.

Hooke found that n was 1.65, while A varied with ice type as anticipated (i.e. fabric influences), being 2.8, 5.0, and 4.5 for white, coarse, and fine ice respectively at -10°C . It should be noted that the fabric of ice described by Hooke is extremely variable throughout the ice mass and that crystal orientation can vary in all three directions.

2-4.2 MEIER'S LAW (12)

Meier's law:

$$\dot{\gamma}_{\text{oct}} = 0.018 \tau_{\text{oct}} + 0.13 \tau_{\text{oct}}^{4.5} \quad (2-7)$$

$$(\dot{\gamma}_{\text{oct}} = \sqrt{2} \dot{\epsilon}_D, \tau_{\text{oct}} = 3/\sqrt{2} \sigma_D)$$

was determined by combining field (Saskatchewan glacier which is temperate with ice grain size of 1 to 100 mm) and laboratory results to obtain a two term flow law for temperate glacier ice. Since Meier combined field and laboratory results, and a wide range of stresses and grain sizes were covered, this law seems an appropriate basis for developing a functional flow relationship for glacier ice. A two term law such as Meier proposed may be thought

of as describing the deformation of ice as the sum of two mechanisms which act simultaneously, but independently, to produce flow.

2-4.3 FUNCTIONAL FLOW RELATIONSHIPS

Hooke's and Meier's laws, as shown in Figure 2-3, have been chosen as base laws from which functional flow relationships can be developed covering a full range of glacier ice temperatures. Hooke's law, describing the behaviour of ice at -10°C , forms the base law for developing complete functional forms H_{BTW} (Hooke (Barnes, Tabor, Walker activation energy)) and H_W (Hooke (Weertman activation)). Meier's law at 0°C has been used directly, as shown in Figure 2-3, and also as shown in Figure 2-4 where it has been linearized between the points indicated, to determine functional forms M_1 and M_2 , respectively. To incorporate temperature, the use of the Arrhenius equation with the assumption of appropriate activation energies is required. The Arrhenius relationship, usually written to describe the importance of temperature, is a straight line on a log log plot of temperature and the quantity of interest. In other words, a rate process approach is adopted to describe the thermally activated process of ice flow.

2-4.3a FUNCTIONAL RELATIONSHIPS H_{BTW} , H_W

Hooke's law, which was originally given in terms of Nye's equivalent stress and equivalent strain rate,

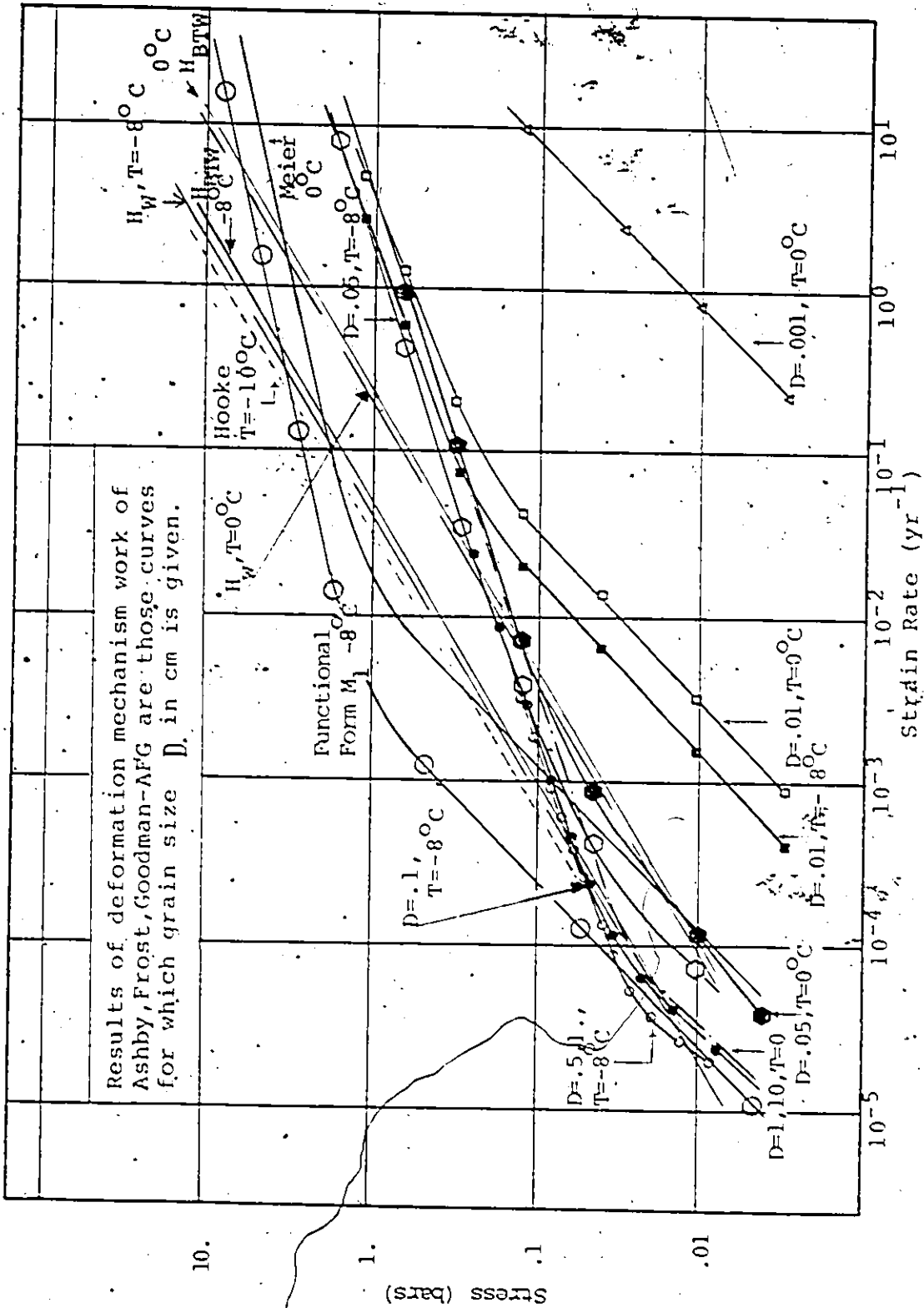


FIGURE 2-3 VARIOUS LAWS

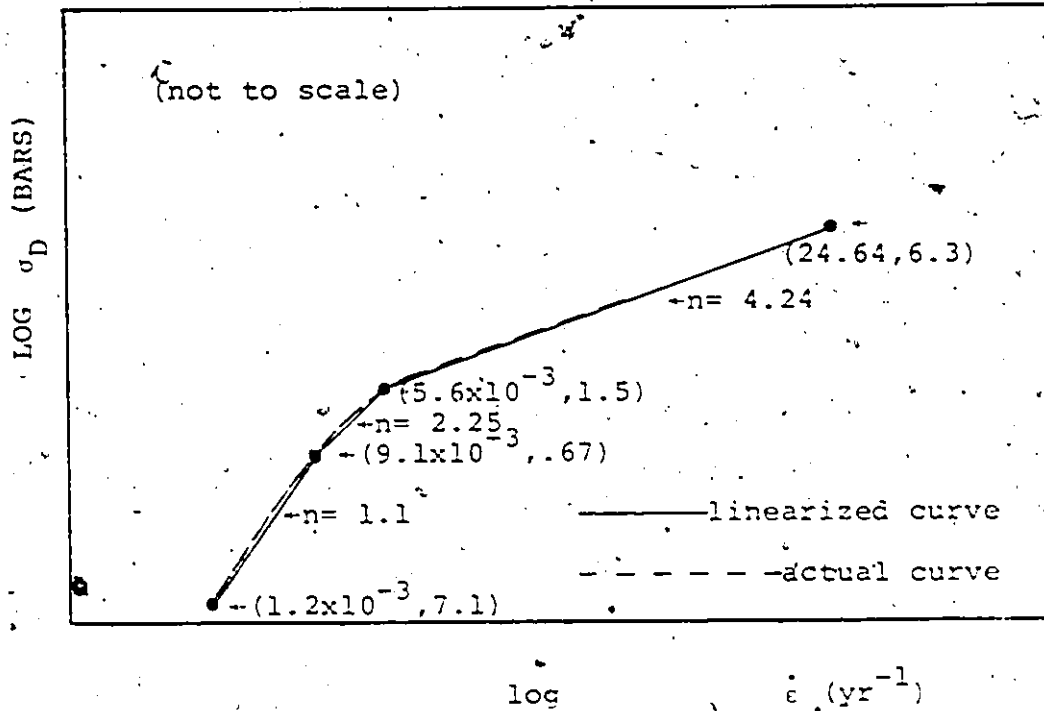


FIGURE 2-4

MEIER'S LAW AT 0°C LINEARIZED

has been converted to Dorn's equivalent stress (σ_D) and equivalent strain rate ($\dot{\epsilon}_D$) yielding:

$$\dot{\epsilon}_D = .4665 (\sigma_D/A)^n \quad (2-8)$$

where n is 1.65 and A is 5.0 bar yr^{1/n}. The assumption of a fixed A implies that the ice is being considered as uniform in this case, i.e. blue ice throughout the Barnes Ice Cap. From rate process theory, the temperature dependence of ice can be written as:

$$\dot{\epsilon}_D = A_L e^{-\Delta E_L/K_B T} c_D^n \quad \text{for } T < -8^\circ\text{C} \quad (2-9)$$

and

$$\dot{\epsilon}_D = A_U e^{-\Delta E_U/K_B T} c_D^n \quad \text{for } T > -8^\circ\text{C} \quad (2-10)$$

where L and U refer to lower and upper temperature ranges, and A , ΔE , K , c , n , and T are defined in Table 2-2. The activation energy is known to vary with temperature as is shown in Table 2-5.

The term:

$$A_L e^{-\Delta E_L/K_B T}$$

is the thermal activation component and is derived from rate process theory considerations. By equating Equations 2-8 and 2-9 at the temperature at which Equation 2-8 was derived, and subsequently solving Equations 2-9 and 2-10 at the temperature where the activation energies change, the functional flow relationship H_{BTW} becomes:

TABLE 2-5
ACTIVATION ENERGY

Barnes, Tabor, Walker (42) - BTW, Weertman (50) - W

Temperature Range °C	BTW		Designation	W
	ΔE KJ/mole	EV		ΔE KJ/mole
-2 to -8	120.0	1.26	ΔE_L	120.0
-8 to -14	78.1	.82	ΔE_L	60.04
-14 to -22	78.1	.82	ΔE_L	60.04

$$\begin{aligned} \dot{\epsilon}_D &= 1.674 \times 10^{14} e^{-9518.39/T} \sigma_D^{1.65} & T_C \leq -8^\circ\text{C} \\ \text{and } \dot{\epsilon}_D &= 3.870 \times 10^{22} e^{-14624.9/T} \sigma_D^{1.65} & T_C \geq -8^\circ\text{C} \end{aligned} \quad H_{BTW} \quad (2-11)$$

where σ_D is in bars and $\dot{\epsilon}$ in year^{-1} . Lower activation energies given by Weertman (50) have also been considered since they may give more realistic results (see Table 2-5). The functional flow/relationship H_W becomes:

$$\begin{aligned} \dot{\epsilon}_D &= 2.635 \times 10^{10} e^{-7215.8/T} \sigma_D^{1.65} & T_C \leq -8^\circ\text{C} \\ \text{and } \dot{\epsilon}_D &= 3.622 \times 10^{22} e^{-14624.9/T} \sigma_D^{1.65} & T_C \geq -8^\circ\text{C} \end{aligned} \quad H_W \quad (2-12)$$

Obviously, the activation energies applicable for ice flow studies must receive further research emphasis.

2-4.3b FUNCTIONAL RELATIONSHIPS M_1 AND M_2

A similar development based on Meier's law at 0°C using the Barnes, Tabor, and Walker activation energies yields the functional flow relationship M_1 :

$$\begin{aligned} \dot{\epsilon}_D &= (2.144 \times 10^{21} \sigma_D + 1.114 \times 10^{21} \sigma_D^{4.5}) e^{-14628.9/T} & T_C \geq -8^\circ\text{C} \\ \text{and } \dot{\epsilon}_D &= (9.278 \times 10^{13} \sigma_D + 4.819 \times 10^{13} \sigma_D^{4.5}) e^{-9518.39/T} & T_C \leq -8^\circ\text{C} \end{aligned} \quad M_1 \quad (2-13)$$

This form of development can be used for any appropriate activation energies.

The second method used to develop a functional flow law from Meier's original work is to use the linearized form given in Figure 2-4. If several deformation mechanisms are known to act, the region over which one of

them is dominant can be represented by a flow law of the form:

$$\dot{\epsilon}_D = A \dot{\epsilon}^n \quad (2-14)$$

over the appropriate region, and by a similar development over all regions. To maintain a close fit to Meier's original curve, the relationship was linearized in three parts as shown in Figure-2-4. This implies interaction of the mechanisms in the transitional region of the curve. The functional flow relationship, M_2 , for this representation is then:

$$\dot{\epsilon}_D = A(\sigma) \dot{\epsilon}^{n(\sigma)} e^{-\Delta E/K_B T} \quad (2-15)$$

where A and n are dependent on stress level as given in Table 2-6 for the Barnes, Tabor and Walker activation energies.

Comparing the functional forms shown in Figure 2-3 to the observed data in Figure 2-2, it can be seen that the functional laws lie in much the same region as the observed data. Exact agreement will not be possible because of the many variables that were not controlled in the tests such as grain size or age. In fact, these specific functional forms were chosen because it was considered that the Hooke and Meier's flow laws are most representative of the field conditions. Had a base flow

TABLE 2-6

FUNCTIONAL FORM M_2 FROM

$$\dot{\epsilon} = A(\sigma) \sigma^{n(\sigma)} e^{-AE/K_B T}$$

STRESS RANGE (Bars)	n	A	
		0°C to -8°C	-8°C to -45°C
0.1 - 0.67	1.1	2.53×10^{21}	1.095×10^{13}
0.67 - 1.5	2.25	4.00×10^{21}	1.735×10^{13}
1.5 - 6.3	4.24	1.79×10^{21}	2.101×10^{12}

law been chosen from some other work in which laboratory results are more representative of the field conditions of interest, it would still not be expected that this law could be applied universally. When a functional flow relationship is being developed, consideration of all the factors thought to be important in the field will lead to the choice of the best available base law to start from.

2-5 FLOW RELATIONSHIPS FOR ICE DEVELOPED FROM MICRO-MECHANISTIC CONSIDERATIONS

Ice has a regular, repetitive array of molecules in its crystal structure, and it is the imperfections in this structure which allows creep deformations under shear. Details concerning the types of imperfections (point, line, interfacial or bulk) will not be given here, but rather their use by Ashby, Frost and Goodman to develop a flow relationship will be discussed (27, 28, 62). For the reader interested in a summary treatment of dislocations, defects and deformation, Appendix 2 has been included covering these topics.

The influence of grain size, aging, barriers, and impurities can also be predicted based on theoretical considerations, and in this regard Ashby, Frost and Goodman have examined the influence of impurities (62). Ashby, Frost, and Goodman considered the various possible mechanisms

which describe the deformation behaviour of ice - dislocation creep, diffusional creep, dislocation glide - and found that the strain rate is given by the sum of the strain rates of the various mechanisms (27, 28, 62). They also gave maps in terms of homologous temperature and normalized stress showing the regions in which given deformation mechanisms are dominant.

The flow relationship they suggested (with substitution of appropriate activation energies, atomic volume, etc. as given in Table 2-7) which is termed AFG in this study is given by:

$$\dot{\epsilon}_D = 1.732 \times 10^{-6} e^{-3916(1-c_s/G)^2/T} + 7.21 \times 10^{-18} e^{-7195.98/T} (c_s/G)^3 (1 + 50(c_s/G)^2 \frac{e^{-4746.8/T}}{e^{-7195.6/T}}) + 1.096 \times 10^{-4} c_s (e^{-7195.6/T}) / T d^2 (1 + \frac{2.8274 \times 10^{-7} e^{-4746.8/T}}{e^{-7195.6/T}}) \quad (2-17)$$

where $\dot{\epsilon}_D$ (yr^{-1}) is Dorn's equivalent strain rate, T is the absolute temperature, G is the shear modulus, d is the grain size, and c_s is $c_D/3$ (bars). Based on Equation 2-17, the strain rate for ice has been evaluated for various temperatures and grain sizes, and these strain rates have been given as a function of stress in Figure 2-3 along with the functional forms, H_{BTW} , H_W , and M_1 . The AFG predicts faster rates. The largest difference between functional flow laws and AFG is about four orders of magnitude over

TABLE 2-7

TYPICAL MICRO-DEFORMATION PARAMETERS FOR ICE

Parameter	Description	Reference	Value
Ω cm ³	Atomic volume	28	3.27×10^{-23}
b cm	Burger's vector	18	4.52×10^{-8}
$T_m^{\circ}K$	Melting temperature	-	273.16
G dynes/cm ²	Shear Modulus	63	$10^{12}/2(14.82-1.317 \times 10^{-2} T_C + 1.034 \times 10^{-5} T_C^2)$
D_{ov} cm ² /sec	Volume Diffusion*	18	11
Q_o ev	Volume Diffusion	18	.62
D_{ob} cm ² /sec	Boundary Diffusion*	18	11
Q_{ob} ev	Boundary Diffusion	28	.409
δ cm	Grain boundary thickness	28	$.9 \times 10^{-7}$
D_{oc} cm ² /sec	Dislocation core diffusion*	28	11
Q_{ob} ev	Dislocation core diffusion	28	.409

* $D_v = D_{ov} \exp(-Q_v/KT)$, $D_b = D_{ob} \exp(-Q_b/KT)$, $D_c = D_{oc} \exp(-Q_c/KT)$

(cont'd....)

TABLE 2-7

TYPICAL MICRO-DEFORMATION PARAMETERS FOR ICE (Continued)

Parameter	Description	Reference	Value
n	Power	28	3.0
A	Dimensionless	28	5.74×10^2
τ_p dyne/cm ²	Peierls stress	28	3.4×10^{10}
ΔF_K ev	Activation For Kink	28	.3375
γ_p cm/sec	Constant	18	10^{-6}
K_B	Boltzman constant	-	8.6164×10^{-5}

the range of temperatures and stresses of interest. However, it should be noted that the grain size of the ice from which the base laws for the functional flow laws were derived, and the grain size used in the AFG flow law form, also varied by at least this order of magnitude. For a grain size of 10 or 100mm, the AFG predictions agree quite well with the observed results in the low stress range.

2-6

SUMMARY

Flow laws based on both empirical and theoretical considerations have been examined to develop essentially five functional stress-strain rate flow laws for glacier ice:

$$\begin{aligned}
 & \dot{\epsilon}_D = 1.674 \times 10^{14} e^{-9518.39/T} \dot{\epsilon}_D^{1.65} \quad T_C \leq -8^\circ\text{C} \\
 H_{\text{BNW}} \left\{ \begin{aligned} & \dot{\epsilon}_D = 3.870 \times 10^{27} e^{-14624.9/T} \dot{\epsilon}_D^{1.65} \quad T_C \geq -8^\circ\text{C} \\ & \dot{\epsilon}_D = 2.635 \times 10^{10} e^{-7215/T} \dot{\epsilon}_D^{1.65} \quad T_C \leq -8^\circ\text{C} \\ H_W \left\{ & \dot{\epsilon}_D = 3.622 \times 10^{22} e^{-14624.9/T} \dot{\epsilon}_D^{1.65} \quad T_C \geq -8^\circ\text{C} \end{aligned} \right. \\
 M_1 \left\{ \begin{aligned} & \dot{\epsilon}_D = (2.144 \times 10^{21} \dot{\epsilon}_D + 1.114 \times 10^{21} \dot{\epsilon}_D^{4.5}) e^{-14624.9/T} \quad T \geq -8^\circ\text{C} \\ & \dot{\epsilon}_D = (9.278 \times 10^{13} \dot{\epsilon}_D + 4.819 \times 10^{13} \dot{\epsilon}_D^{4.5}) e^{-9518.39/T} \quad T \leq -8^\circ\text{C} \end{aligned} \right. \\
 M_2 \left\{ \begin{aligned} & \dot{\epsilon}_D = A(\sigma) \sigma^{n(\sigma)} e^{-\Delta E/K_B T} \\ & \text{(Table 2-6)} \end{aligned} \right.
 \end{aligned}$$

$$\begin{aligned}
 \text{AFG } \dot{c}_D &= 1.732 \times 10^{-6} e^{-3916(1-(c_s/G)^2)/T} + \\
 & 7.21 \times 10^{-18} e^{-7195.58/T} (c_s/G)^3 (1 + 50(c_s/G)^2 \frac{e^{-4746.8/T}}{e^{-7195.58/T}}) + \\
 & 1.096 \times 10^{-4} c_s e^{-7195.58/T} (1 + \frac{2.8274 \times 10^{-7} e^{-4746.8/T}}{e^{-7195.58/T}}) / T d^2
 \end{aligned}$$

While discrepancies obviously exist between predicted and observed rates (Meier, Hooke) as indicated in Figure 2-3, given the idealizations made and the randomness of actual glacier ice, the functional forms of the ice flow laws show great promise for use in simulation programs. To improve the functional forms, factors such as ice fabric, aging, orientation, and so on, should be included. The functional forms of the ice flow laws can be readily modified to incorporate such considerations as the necessary research is completed to provide the appropriate constants (e.g. activation energy). In this regard, theoretical (micro-mechanistic) considerations of Ashby, Frost and Goodman have lead to a better understanding of the parameters influencing ice flow.

CHAPTER 3

INFLUENCE OF INITIAL STRESSES

3-1

INITIAL STRESSES

The solution of time dependent boundary value problems requires a knowledge of both the initial and boundary conditions. During the flow analysis of ice masses, the initial stresses can play an important role as most flow relationships for ice are stress dependent. Customarily in the study of large ice masses with relatively flat surfaces it is assumed that flow is due to the shear stress τ (Equation 2-3) acting at any depth. Obviously, using this assumption for τ implies that the normal stress influences are not significant (i.e., $\sigma_H = \sigma_V$ for small σ_s and Poisson's ratio $\nu = .5$) and that the bedrock profile is similar to the surface profile. These assumptions that were made for ease of analytical treatment in the past can introduce significant errors. However, such simplifying assumptions are not necessary in the finite element method.

The "retention" of lateral stress states due to previous vertical stresses is well recognized in geotechnology. For instance, the maximum past effective vertical pressure (preconsolidation pressure) a soil sustained due to

previous conditions can often be determined through consolidation tests (64) and knowledge of this pressure is critical in settlement problems. This has also been shown for typical rock squeezing problems under high lateral stresses ($\sigma_H \gg \sigma_V$) in Southern Ontario (65). Similarly, it would seem reasonable for ice, that influences of previous stress states might also be retained. (Also termed remnant stress states in this study.) This possibility and its influence is considered in this Chapter.

In the finite element analysis, such stress states can be considered if their levels and extent are known. Many valley glaciers, which are common in Canada and Europe, have been receding in the past century with their firm limit retreating to higher altitudes. This recession may have caused some unloading of such ice masses. The most pronounced case of glacier recession, and the associated reduction of vertical stresses, is the world's ice caps which have been much larger in the past. For this reason, remnant lateral stresses may be influencing the flow of these glaciers.

This should be contrasted with the usual assumptions that the surface slope determines the shear stress. In considering the influence of initial stresses using the finite element method approach, two general cases were considered: 1) elastic stresses under self weight which has been the usual approach to date; and 2) remnant initial stresses

of various magnitudes. The various stress states are dealt with in the following section.

In this Chapter, two different finite element formulations are also compared. The formulation which has been used most often to date is a small deflection theory approach using a fully explicit scheme based on the incremental, initial strain method, and termed E here (1,2,3,24). The second formulation, developed by Mirza (66) for the simulation of ice mass flow, uses either small or large deflection theory and an implicit scheme to solve ice mass flow problems. This approach will be termed I here (66,67,68,69). The two finite element method formulations have been used to simulate the same problem, and the solutions compared to determine the relative merit of the two simulation methods. It must be noted that the stress states assumed are hypothetical and that superposition is not implied.

3-2

STRESS STATES ASSUMED

The shear stress as a function of surface slope is often used in glaciological work, and this is discussed briefly in the previous section. The second common assumption for the stress state acting is that it is the elastic stress state under self weight as shown in Figure 3-1a. When the horizontal and vertical stress levels are the same with no shear stresses on these planes (level ground with $\nu=0.5$), Figure 3-1a becomes Figure 3-1b, the hydrostatic case. If remnant stresses exist, then the total stresses are not functions of the depth alone, and no simple relationship between the stresses can be derived

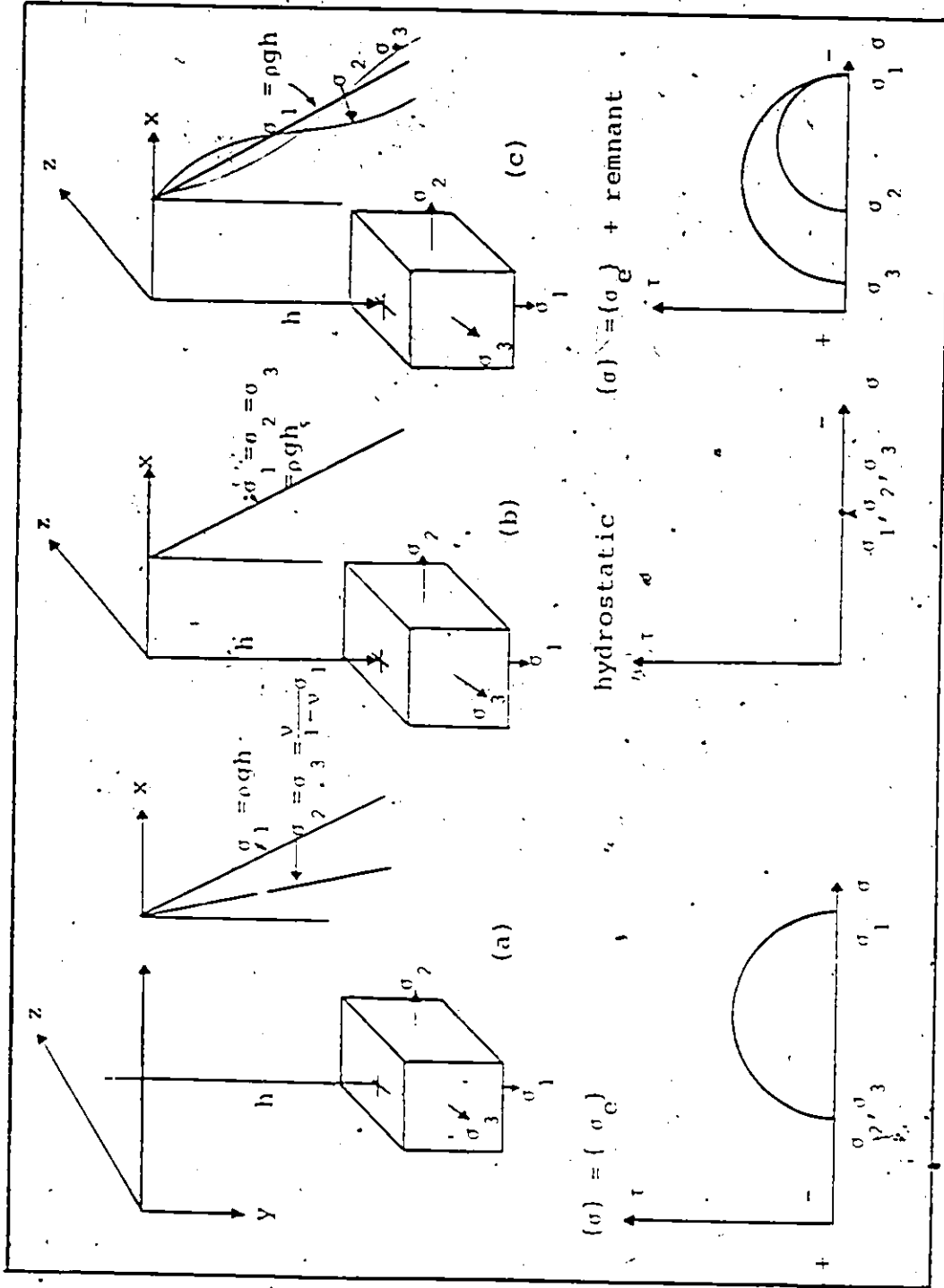


FIGURE 3-1 STRESS STATES

analytically (Figure 3-1c). In this case field measurements are required to determine the in situ stress levels. Although fabric is indicative of a "memory" of past history, it was assumed previously that remnant stresses (if they exist) would dissipate rapidly because the relaxation time of ice is small compared to the time span involved with glaciological events.

Thus, it would seem reasonable to assume that the gravity stress state or one close to it, prevails. However, early in this study and during previous work by Hanafy(5), two aspects of potential concern were recognized: 1) If they do exist, remnant stresses would significantly influence glacier flow rates, particularly with regard to surging; and 2) Remnant stresses would be responsible for part of the apparent lack of agreement between measured and predicted flow rates when appropriate flow relationships and initial gravity stress states have been assumed.

Given these problems, it was evident that remnant stress state influences must be investigated in detail, with final resolution of their importance depending on improved field measurements of stress conditions in actual ice masses. Two distinct potential problems have been identified here - flow relationships and initial stress conditions - and both are critical to realistic ice mass flow simulation. Indeed, the problem is one of determining the glacier stresses or strains as an initial condition at the time the flow analysis is initiated

($t = 0$ for analysis in a finite element program is just a point in time as far as the glacier is "concerned").

The potential influence of remnant stress states was dealt with in two different ways. In the first case, designated S_1 , the remnant stress levels were given simply as a function of the vertical stress:

$$\sigma_H = K\sigma_V \quad (3-1)$$

but it was felt that this could lead to some problems as this concept borrowed from soil mechanics is not really applicable for sloping ground. For this reason, the remnant stresses (assumed to be lateral) were considered in case S_2 to be given by:

$$\sigma_H = K \sigma_x^e \quad (3-2)$$

where σ_x^e is the elastic horizontal stress and K is a multiplier introducing a perturbation from the elastic case, i.e.:

$$K = 1 + \alpha \quad (3-3)$$

where α is the perturbation factor. The shear stress from the elastic self weight solution was used throughout.

Once the stress state is determined it is necessary in the finite element method solution to determine the strains. In this study, the strains (elastic, plastic, creep) could be dealt with in a variety of ways. However, only two were

$$\sigma_H = \sigma_x^e + \alpha \text{ remnant} = \sigma_x^e + \alpha \sigma_x^e = (1 + \alpha) \sigma_x^e$$

considered here as shown schematically in Figure 3-2:

1. The remnant strains are not recoverable and generally unknown (-U).[¶] For simplification the initial strain state is taken to be the elastic strain due to self weight. However the remnant stresses are assumed to influence flow and the initial stress state is the remnant stresses plus the self weight stresses.
2. The remnant strains are recoverable and related to the remnant stresses by elasticity (-R-).[¶] The initial stress state is the remnant stresses plus self weight stresses as above.

The first case was used in reporting results for this study as it appears the more reasonable, although both schemes were employed initially.

3-3 TYPICAL ICE MASS AND STEADY STATE FLOW

Three finite element meshes, for a hypothetical ice slope with break, symmetrical about AB as shown in Figure 3-3, were used to study the influence of initial stresses. The various stress levels and the schemes used in the finite element method flow simulation of the large ice masses is given in Table 3-1.

To determine the influence of initial stress states on the behaviour of large ice masses, the steady state finite element method solutions for the various initial remnant stress cases have been compared in terms of equivalent stresses and surface

[¶] -U- Unknown, -R- Recoverable.

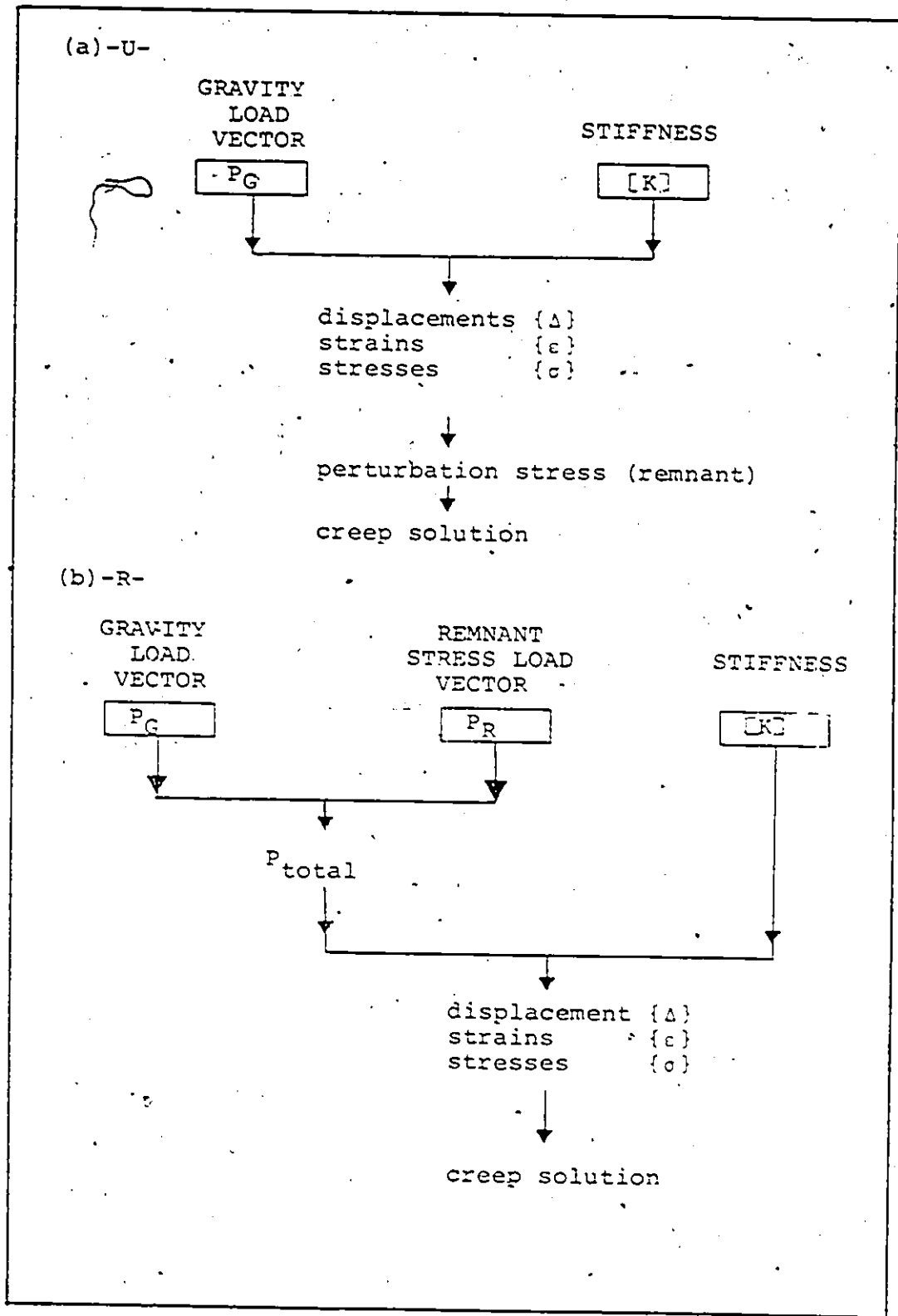


FIGURE 3-2
STRAIN SCHEMES

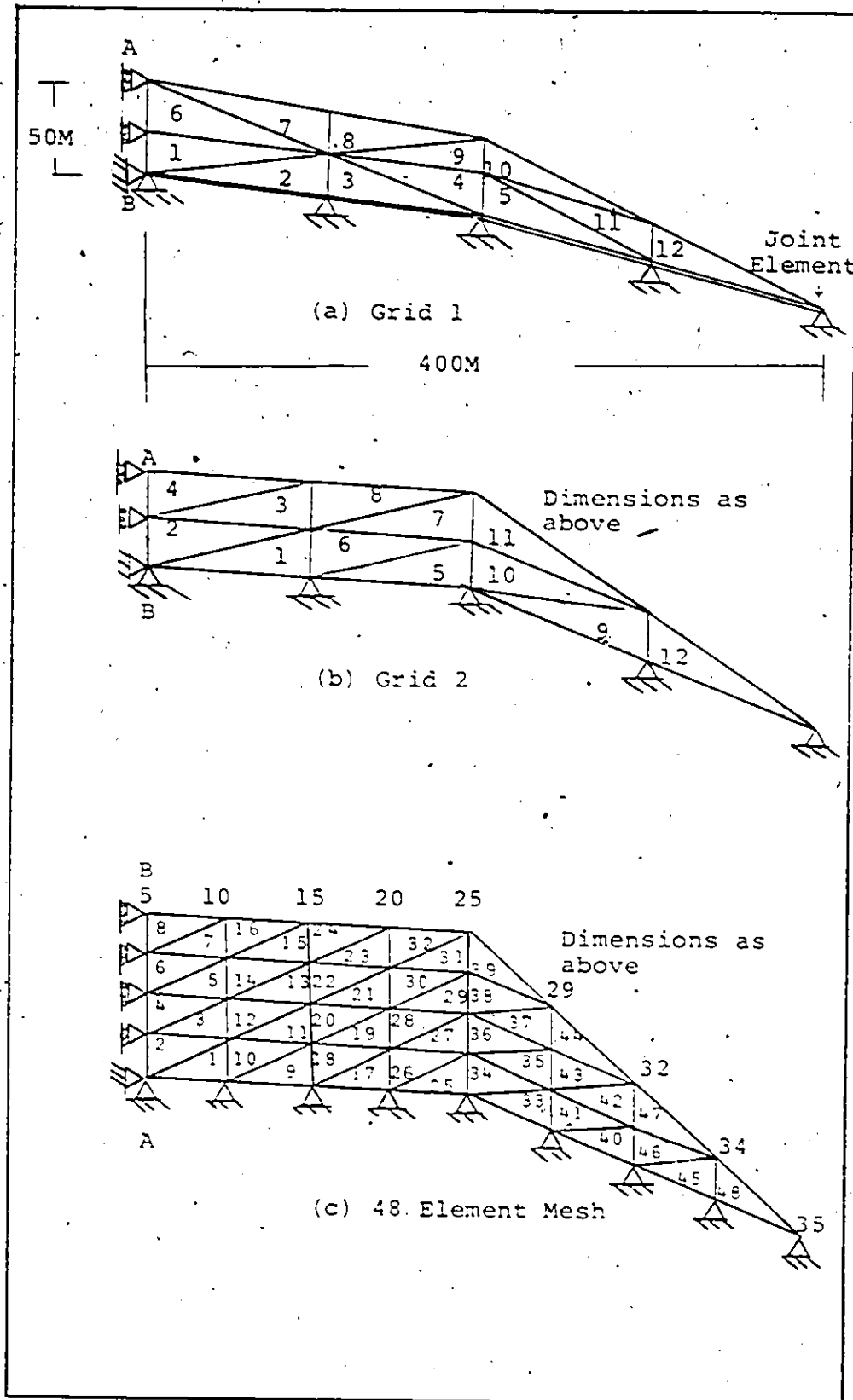


FIGURE 3-3 ICE MASS STUDIED (THREE REPRESENTATIONS)

velocities. Steady state has been considered to be the condition when the strain rates are essentially constant for each element, i.e. the equivalent stress is no longer changing significantly.

If the steady state finite element method solution after a reasonable time is not influenced significantly by the initial stress conditions assumed (i.e. relaxation of locked-in stresses), then for the finite element method simulation of glacier flow problems, the gravity state of stress can be used as the initial condition. If the influence of initial stresses is significant, then the entire glaciological history, or the state of stress at the beginning of the analysis, must be determinable (i.e. field measurements of stress, or flow rates which are back solved for stresses) for use in the finite element method simulation.

3-4

RESULTS

In this section, the steady state finite element method solutions of large ice mass flow problems are presented and compared. The typical ice masses given in Figure 3-3 as well as the Barnes Ice Cap were modelled using the finite element method described previously by other researchers (4,5). The results will be discussed in conjunction with Table 3-1.

In Figure 3-4 the equivalent stress is shown as a function of time for Element 10. The equivalent stresses (cases 1 to 5) illustrated, at first very different, have become

TABLE 3-1
 STRESS STATES AND SCHEMES
 USED IN SIMULATION
 (All use -U- Assumption)

Case	σ_x e- elastic	σ_y	τ_{xy}	Mesh Figure 4-3	Approach Implicit I Explicit E	Stress $\sigma_H = K\sigma_y - S_1$ $\sigma_H = K\sigma_x - S_2$	Figure
1	0.5e	e	e	a	E	S_1	3-4
2	0.75e	e	e	a	E	S_1	3-4
3	1.00e	e	e	a	E	S_1	3-4
4	2.00e	e	e	a	E	S_1	3-4
5	e	e	e	a	E	S_1	3-4
6	e	e	e	c	E	S_1	3-5,6
7	0.5e	e	e	c	E	S_1	3-5,6
8	0.75e	e	e	c	E	S_1	3-5,6
9	1.00e	e	e	c	E	S_1	3-5,6
10	1.01e	e	e	c	E	S_1	3-6

(Cont'd.....)

TABLE 3-1 (Continued)

Case	σ_x	σ_y	τ_{xy}	Mesh	Approach	Stress	Figure
11	1.02e	e	e	c	E	S ₁	3-6
12	1.05e	e	e	c	E	S ₁	3-6
13	2.00e	e	e	c	E	S ₁	3-5,6
14	.5e	e	e	b	F	S ₂	3-7
15	1.5e	e	e	b	E	S ₂	3-7
16	0.5e	c	c	b	I	S ₂	3-8
17	1.50e	c	e	b	J	S ₂	3-8
18	0.25e	e	e	b	I	S ₂	3-8
19	2.00e	e	e	b	I	S ₂	
20	e	e	e	Barnes	E	-	

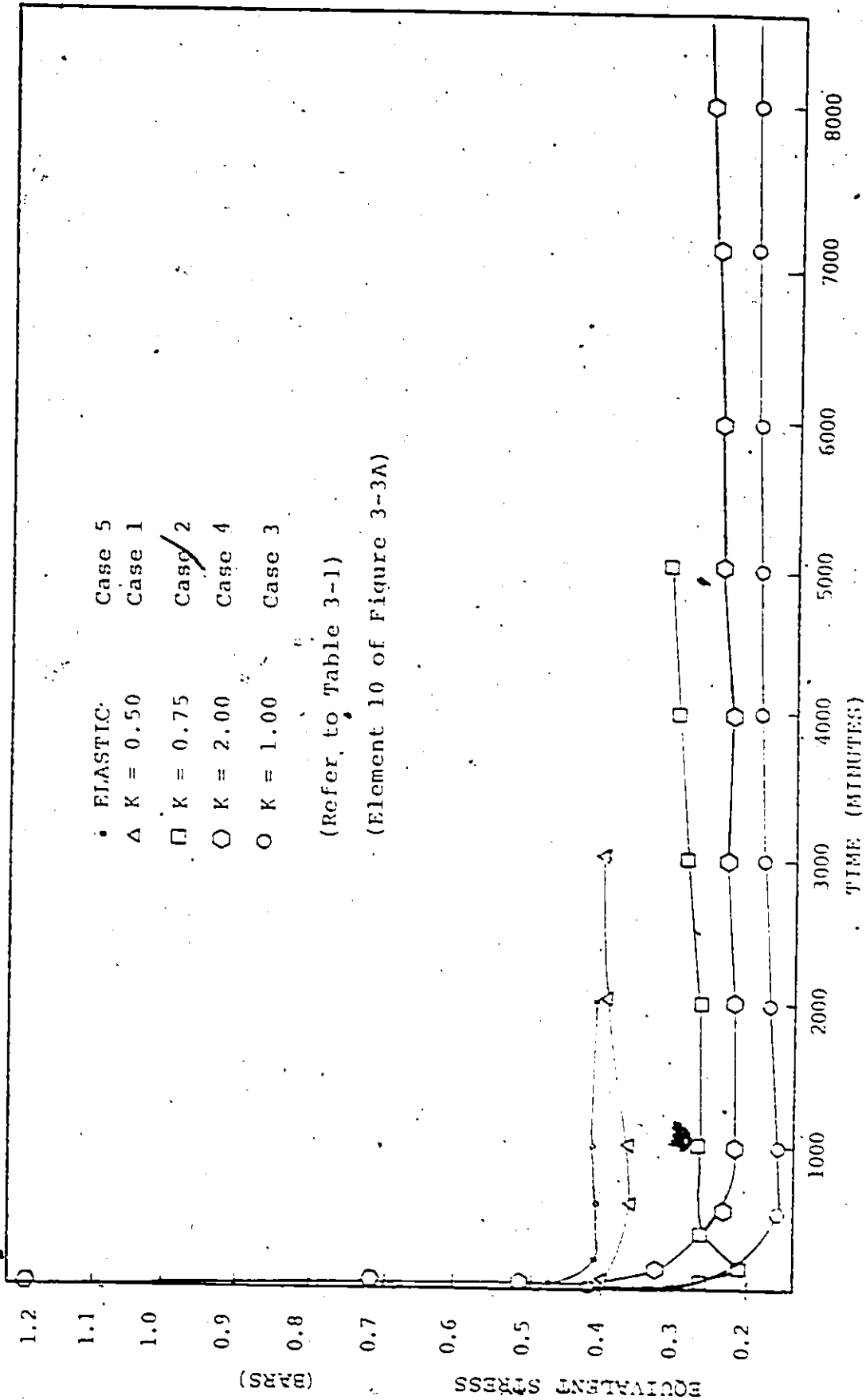


FIGURE 3-4 EQUIVALENT STRESS

somewhat closer at steady state, but do not appear to converge at steady state (history about 5 hours).

Cases 6 to 13, for the more refined grid, have been compared in Table 3-2 and in Figures 3-5 and 3-6. From Figures 3-5 and 3-6, it can be seen that the steady state solution is almost reached. Again the stresses at steady state have not converged. The steady state surface velocities for the various cases are given in Table 3-2. It can be seen that the finite element method surface velocities for different initial conditions are significantly different. In fact, using the S_1 stress scheme the flow has gone uphill for the very high horizontal stress levels due to the assumption that this stress is simply a multiple of the vertical stress.

It can be seen from a comparison of Figures 3-5 and 3-6 that although the equivalent stress has become almost constant, small changes in horizontal stress are still occurring, and steady state may not quite have been reached.

In Figure 3-7 the equivalent stresses are given in several elements for various cases, covering longer flow times (about 3 months) than had previously been completed using the explicit method. The results indicate that the finite element solution for the steady state flow of the ice ramp is finally reached at about 12000 minutes (8 days). Element 12 demonstrates steady state behaviour at about this time, while most other elements appear to reach steady state much earlier. The results

TABLE 3-2 (Cases 6 to 13).
STEADY STATE SURFACE FLOW RATES (M/YEAR)

Case No	Elastic		K = .5		K = .75		K = 1.0		K = 1.01		K = 1.02		K = 1.05		K = 2.00	
	V _x	V _y	V _x	V _y	V _x	V _y	V _x	V _y	V _x	V _y	V _x	V _y	V _x	V _y	V _x	V _y
5	0.00	.15	0.00	.15	0.00	.10	0.00	.066	0.00	0.64	0.00	.063	0.00	.052	-0.00	+.079
10	.17	.13	.16	.13	.10	.087	.061	.055	.059	.054	.057	.052	.052	.019	-.088	+.064
15	.33	.12	.31	.12	.21	.076	.13	.047	.126	.045	.123	.044	.113	.041	-.175	+.056
20	.48	.13	.45	.12	.31	.072	.19	.040	.189	.039	.184	.038	.171	.035	-.244	+.055
25	.62	.15	.58	.13	.39	.076	.24	.040	.235	.039	.230	.038	.214	.034	-.301	+.061
29	.70	.14	.65	.13	.48	.074	.24	.038	.238	.037	.232	.035	.213	.032	-.317	+.062
32	.54	.12	.48	.11	.29	.065	.15	.034	.148	.033	.143	.032	.129	.029	-.229	+.055
34	.35	.073	.30	.06	.18	.036	.093	.019	.090	.019	.087	.018	.079	.016	-.155	+.323
35							Fixed									

V_x + to right, V_y + down.

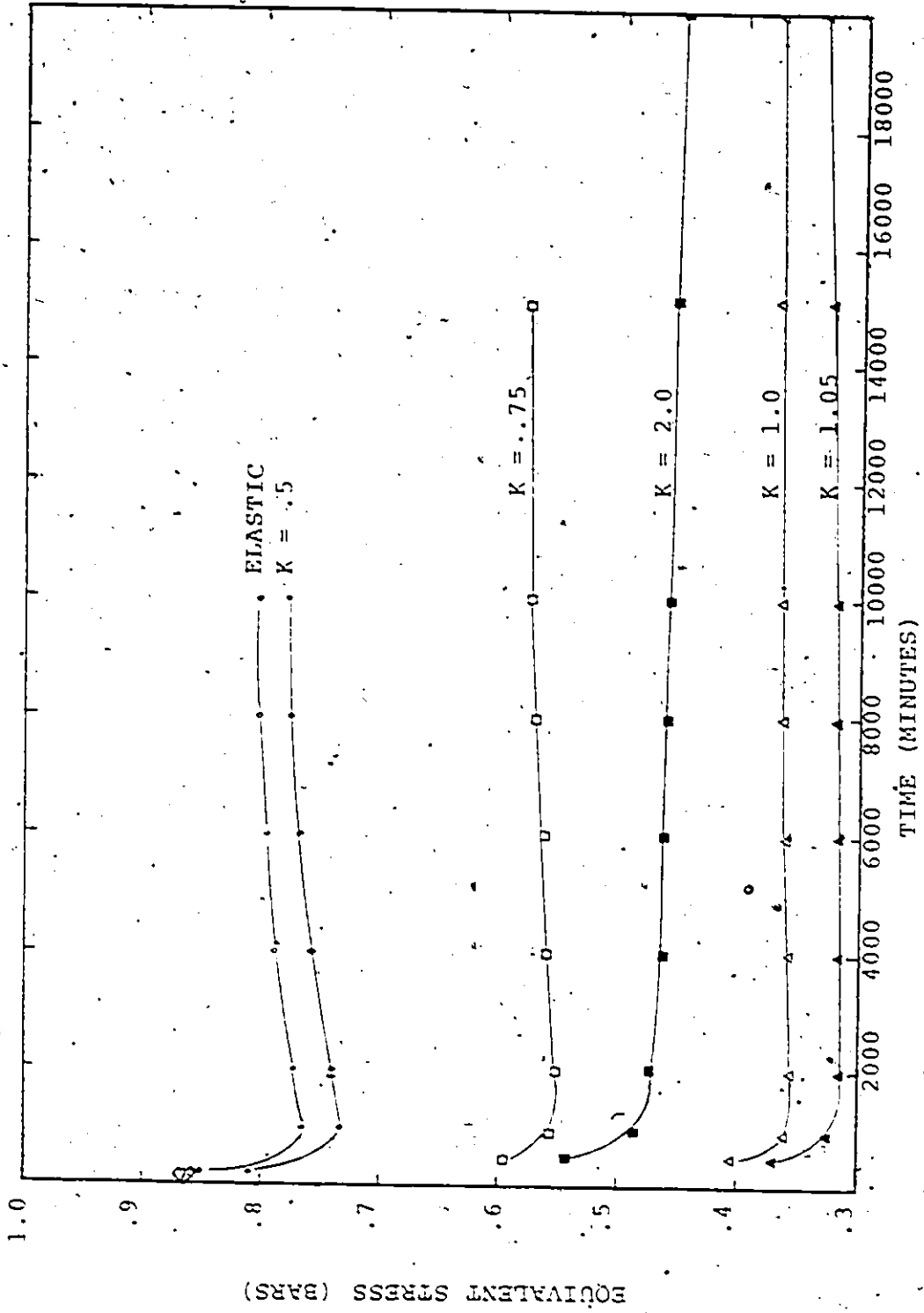


FIGURE 3-5. CASES (6 TO 13) EQUIVALENT STRESS (ELEMENT 43 OF FIGURE 3-3C)

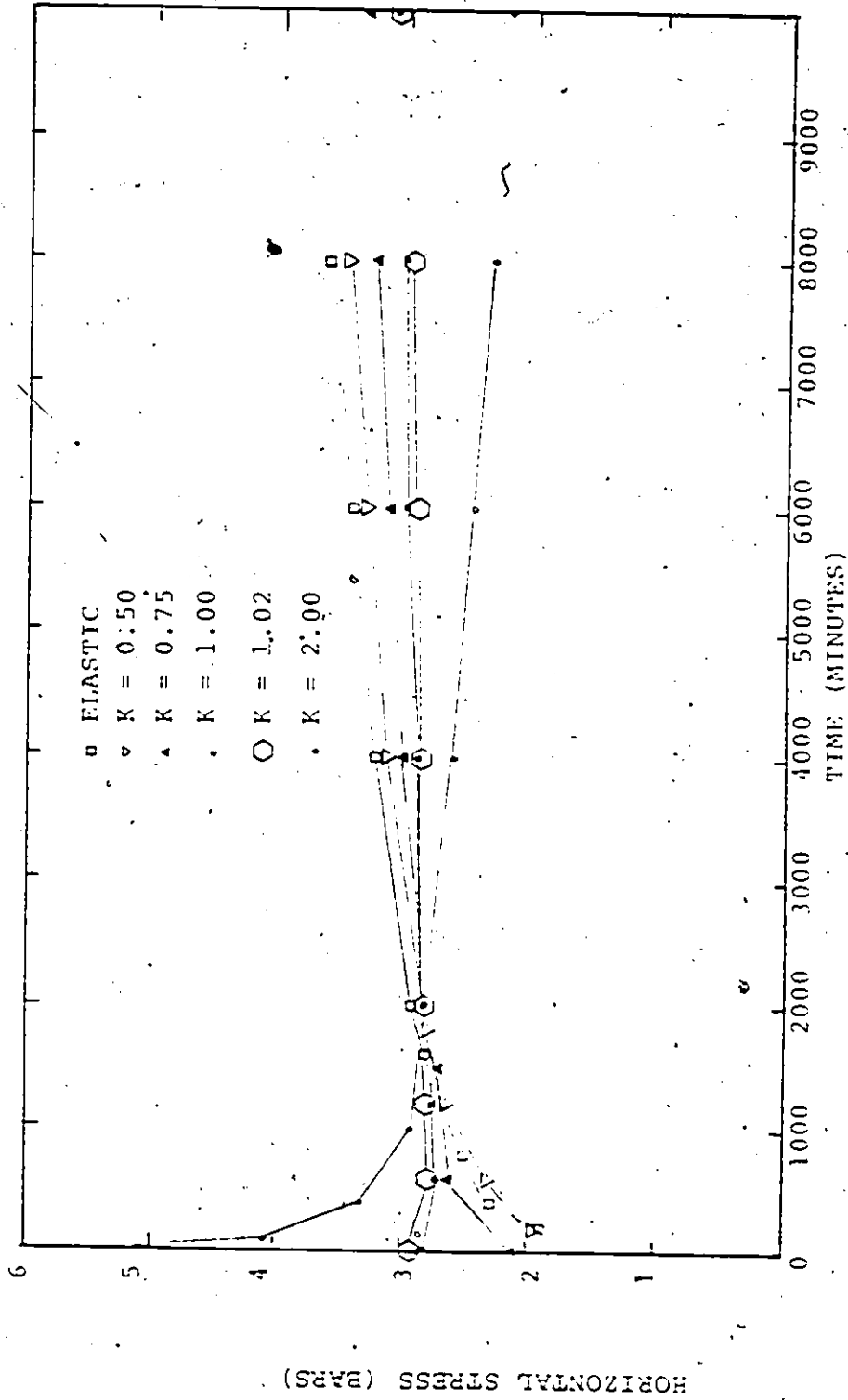


FIGURE 3-6 CASES (6 TO 13) HORIZONTAL STRESS (ELEMENT 11 OF FIGURE 3-3C)

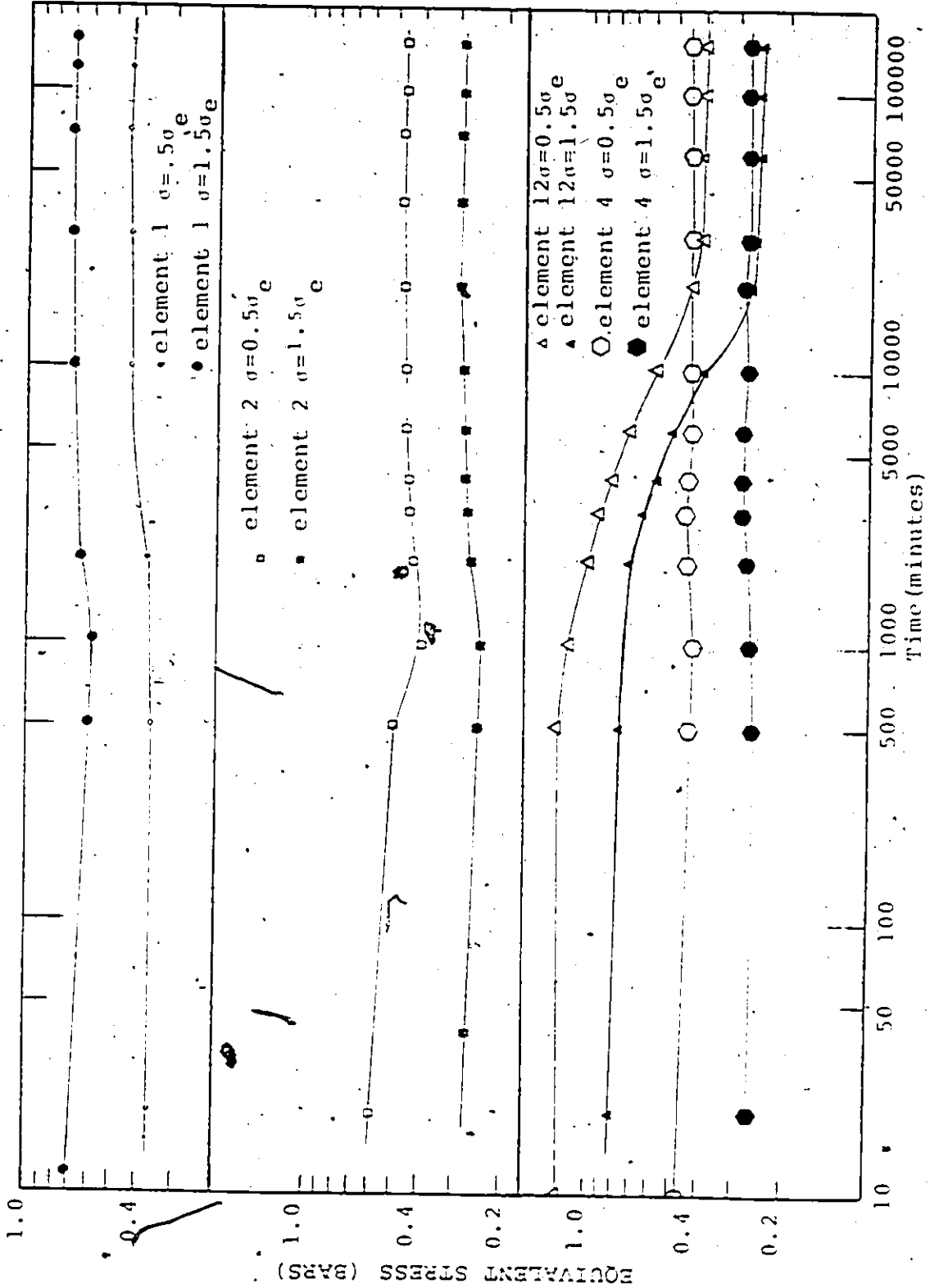


FIGURE 3-7 EQUIVALENT STRESS - EXPLICIT SCHEME, CASES 14 AND 15, VARIOUS ELEMENTS

for the implicit scheme using the same grid are shown in Figure 3-8, and are the same as for the explicit scheme at steady state.

For both the implicit and explicit schemes, the initial stress has significantly influenced the steady state solution, although the difference between the equivalent stresses at steady state is less than the original ($t = 0$) difference. The steady state solution for the explicit scheme can be compared to the steady state solution for the implicit scheme. It can be seen that the steady state stresses predicted by both schemes are identical. Both schemes clearly indicate that the influence of initial stresses, if they exist, is too large to be ignored. To overcome this problem it will be necessary to convert field measurements into meaningful initial conditions for the finite element simulation of ice mass flow.

The flow rates using the explicit scheme for the Barnes Ice Cap were computed previously at McMaster University by Hanafy (5) and are shown in Figure 3-9 for various flow laws. These results show very poor agreement to the observed results, and it is expected that with improved knowledge of potential in situ stresses that the simulation results can be significantly improved.

3-5

SURGING

Glaciers, throughout most of their history, move very slowly. At times however a glacier may advance rapidly for a

* Implicit scheme in development by Mirza at McMaster University, solution unstable at steady state.

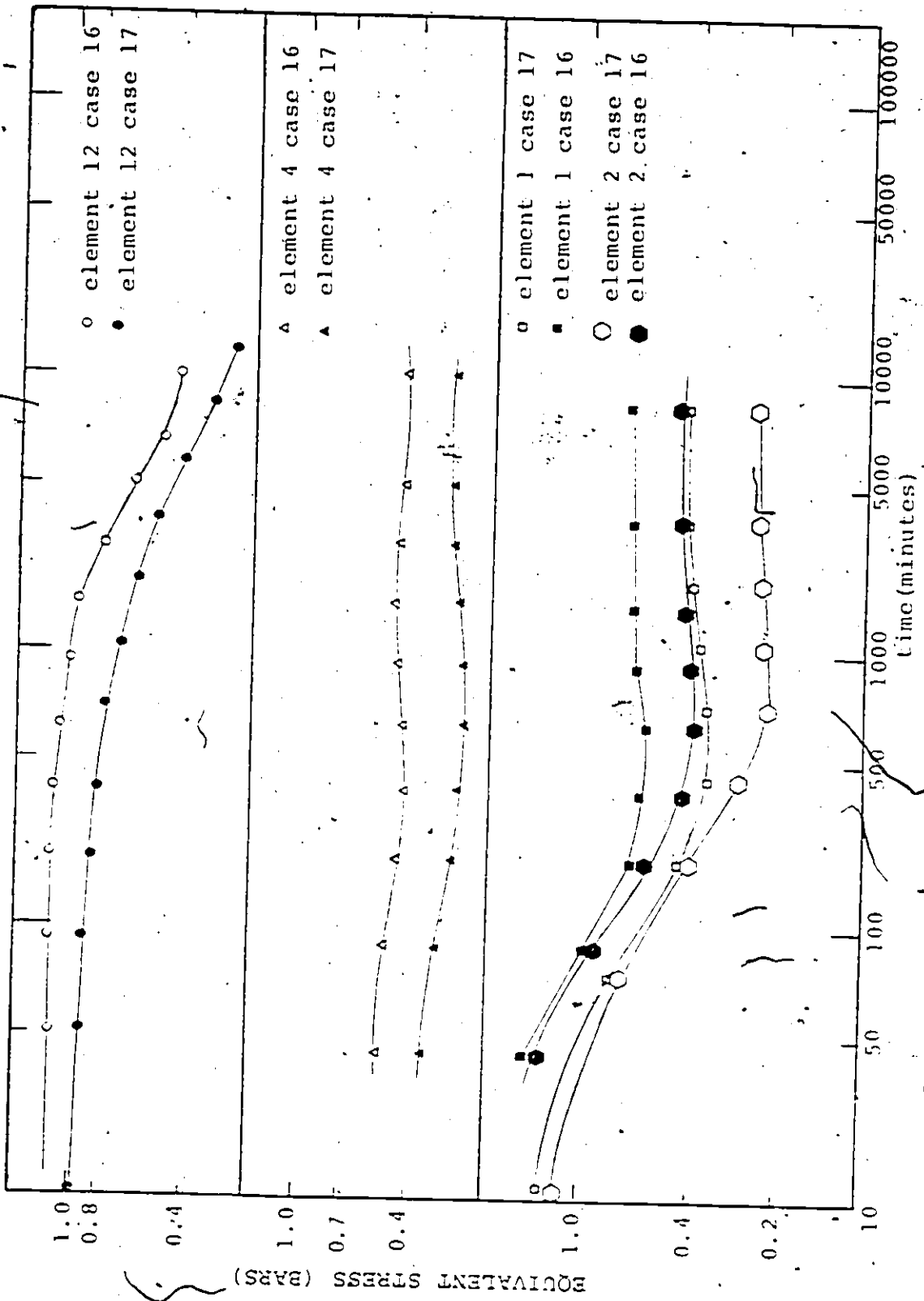


FIGURE 1-8 EQUIVALENT STRESS-IMPLICIT SCHEME, CASES 16 AND 17, VARIOUS ELEMENTS

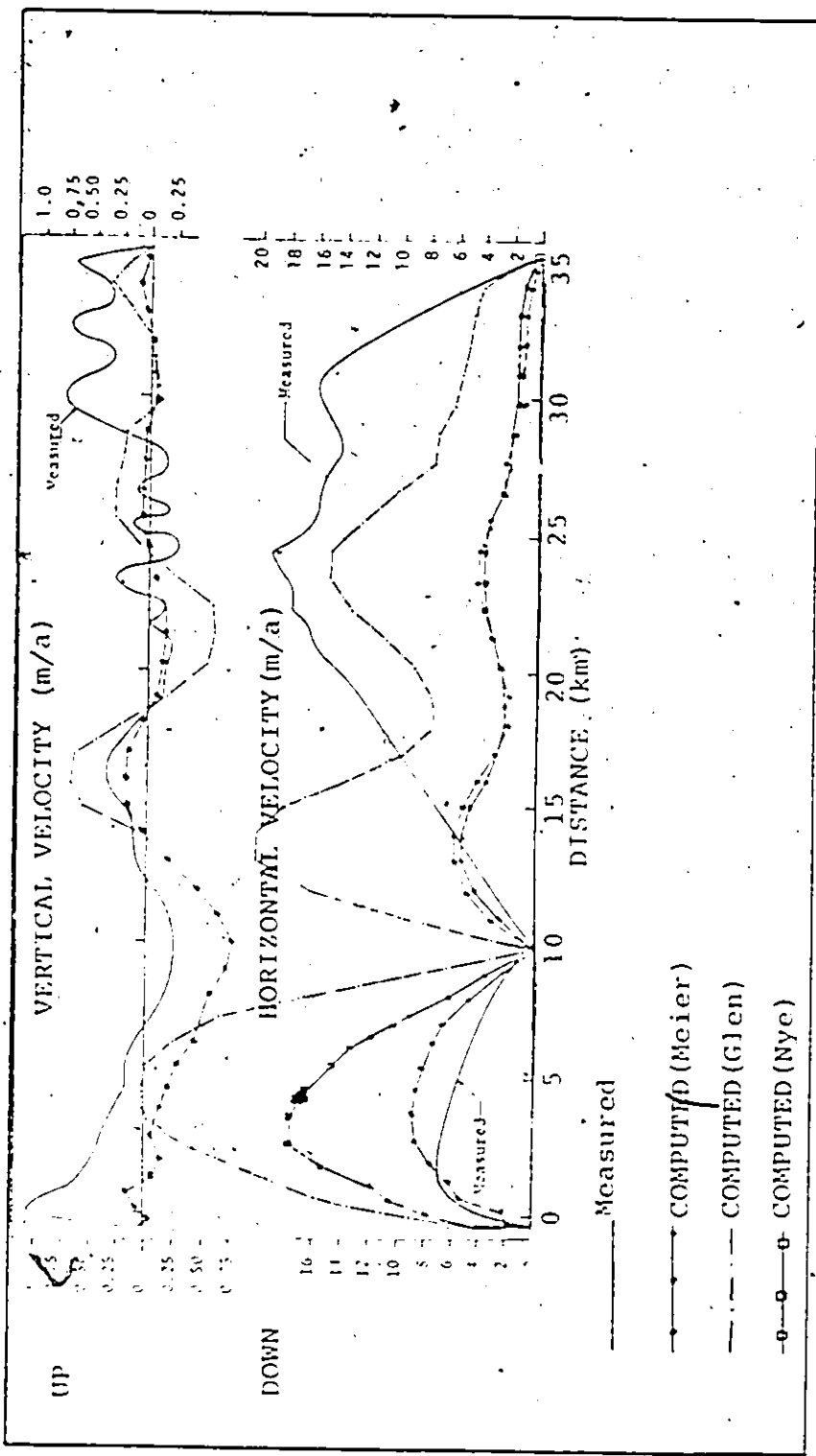


FIGURE 3-9 COMPARISON OF STEADY FLOW RATES, BARNES ICE CAP

short time, called surging (7,70,71), and then start moving slowly again. Surging of whole valley glaciers and parts of ice caps has been known to occur. Nguyen used joint elements as an approach to modelling the surge process (4). However, the conditions which cause surging are not well known, and in fact the debate about surging continues today. However, since surging appears to be an instability problem, a large deflection approach coupled with initial stress considerations and transient thermal conditions may be needed to solve the surging problem. This type of an approach is being developed at McMaster University using input from the study reported here.

3-6 DISCUSSION AND METHODS OF DEALING WITH INITIAL STRESSES

From the results of two formulations which consider the role of initial stress states, it was seen that the usual elastic state of stress under gravity loading assumption is not necessarily the correct initial condition for the finite element method simulation of large ice masses. Perturbations from the elastic stress state indicate that the usual state of stress assumed (gravity) is not a limiting case due to flow, but rather, that the field conditions must be known at the beginning of the simulation.

Several methods of determining the in situ state of stress are possible (typically in glaciology using methods developed by Nye (7,54)), although methods based on field measurements have mainly been used (8). In future simulation

flow rates obtained in the field (care being taken to use the correct flow rates as indicated in Chapter 4) coupled with other boundary conditions will be used to determine the initial stress state, which can then be used to study glacier flow. However, this will also require a detailed knowledge of the appropriate flow relationship as discussed previously.

Since creep inevitably involves geometry changes, a large deflection simulation method seems to be more suited to ice mass flow problems than the current approach. Other conditions such as temperature, still assumed to be isothermal by most researchers (even those using the finite element method (75)), must also be considered along with initial stresses and appropriate flow relationships before significant advances in the art of ice mass simulation will occur. The implicit scheme still needs further work to take it into the complete time domain past the initiation of steady state.



CHAPTER 4

TEMPERATURE INFLUENCES ON GLACIER FLOW

4-1

TEMPERATURE INFLUENCES

Glaciers; typically found at temperatures between 0°C and -60°C , have uniform or non-uniform temperature distributions which may approach steady-state or be transient. In this Chapter, the importance of considering these temperature distributions when simulating glacier flow problems is examined.

A temperate glacier is by definition at, or close to, the pressure melting temperature throughout and moving primarily by basal slip and internal deformation. Correspondingly, a cold glacier is at a temperature lower than the pressure melting temperature throughout, and moving primarily by internal deformation. These two rather broad classifications will be used in this study to describe the ice mass under consideration.

In the previous Chapter, the influence of initial stress was examined using "model" temperate glaciers, while in this Chapter "model" cold glaciers having both uniform and non-uniform temperature distributions are considered. Similarly, a typical cold glacier, the Barnes Ice Cap, representative of Canada's northern ice masses has been modelled.

The temperature distribution for the Barnes Ice Cap was provided by the Glaciology Division of Environment Canada, and is based on observed results and a steady state mathematical model (72). This temperature distribution for the Barnes Ice Cap is given in Figure 4-1. In the more general case, when the temperature distribution of a natural ice mass is sought, a model which includes: a) frictional heat; b) geothermal flux; c) crevassing; d) convection of surface air; e) absorption of radiation; and f) the movement of water, should be used. These factors could then be used in a transient thermal analysis finite element model to predict the temperature distribution of any glacier, although this has not been done here. (Thermal analyses form part of a related current research program.)

It should be noted that due to geothermal flux or frictional heating, ice masses in Northern Canada tend to be warmer at their base than at their surface (for example, Figure 4-1).

4-2

ICE MASSES CONSIDERED.

To determine the influence of temperature on the creep behaviour of ice masses, the glaciers modelled in Chapter Three were used again, but different temperature distributions were adopted (Figures 4-1, 4-2, and 4-3). The Barnes Ice Cap, shown in Figure 4-1, may in fact be at the pressure melting point at the base (ice becomes water)

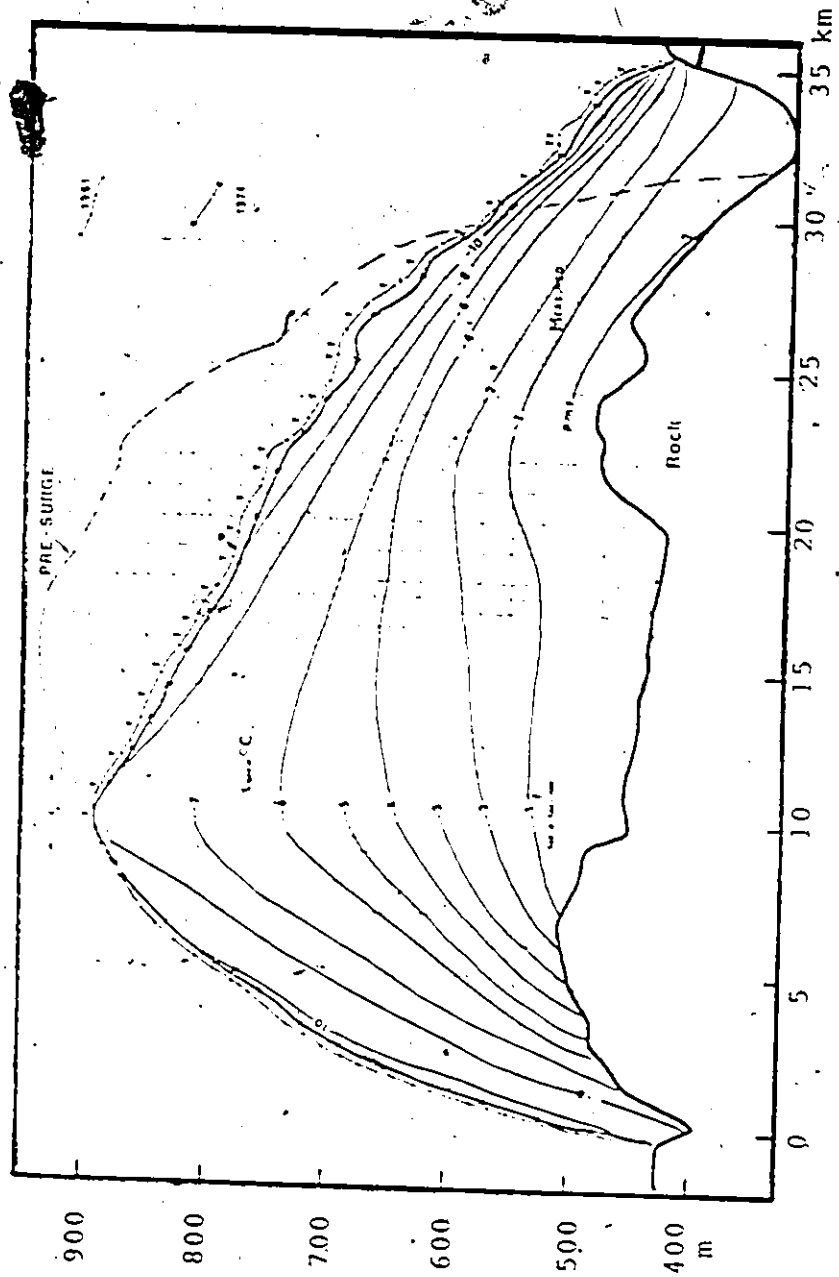


FIGURE 4-1 BARNES ICE CAP TEMPERATURE DISTRIBUTION

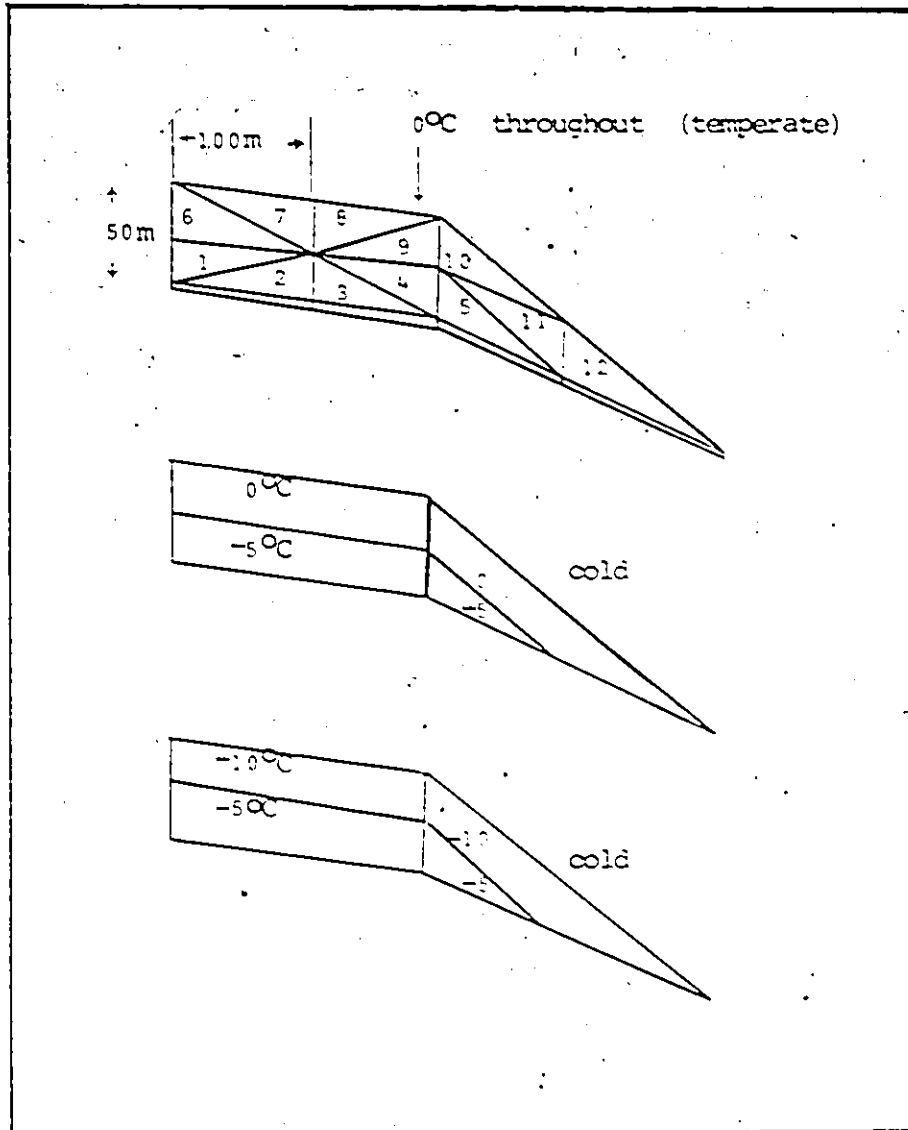


FIGURE 4-2 12 ELEMENT MESH TEMPERATURE DISTRIBUTIONS

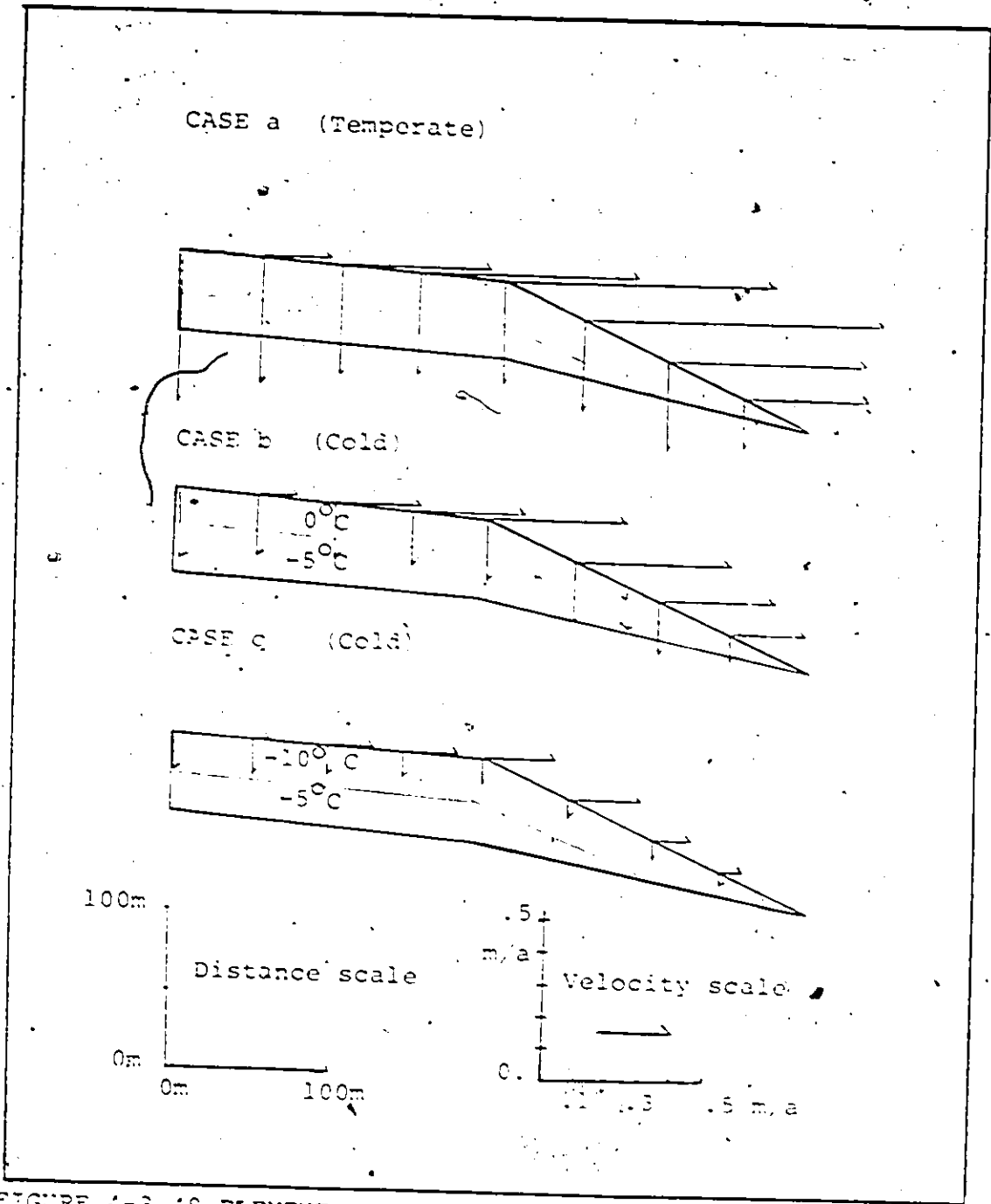


FIGURE 4-3 48 ELEMENT MESH, TEMPERATURE AND VELOCITY DISTRIBUTION

which may lead to surging. The temperature distribution shown for the Barnes Ice Cap has been derived assuming that the divide (locus of stationary points) is fixed in time.

4-3

FLOW RELATIONSHIPS CONSIDERED

Glen's law, Nye's law and functional flow law H_{BTW} were used in conjunction with the 12 and 48 element meshes for the ice mass "models" shown in Figures 4-2 and 4-3. An initial elastic state of stress was assumed. In the case of the more refined grid it was also assumed that the horizontal stress equalled the vertical stress. These two meshes with the temperature distributions and stress states indicated were used to determine the influence of non-uniform cold temperature distributions:

Several laws including the functional forms H_{BTW} , H_W and M_{1BTW} were used in conjunction with the Barnes Ice Cap model given in Figure 4-1. Previously, an isothermal temperature distribution had been assumed during ice flow studies for the Barnes Ice Cap at McMaster University. It was hoped that a more realistic temperature distribution representation would lead to closer correlation between observed and computed steady state velocity distributions from the finite element method analysis. —

4-4

DISCUSSION OF RESULTS

For the steady state flow condition the creep rate, equivalent stress, and surface velocity are constant. To study the influence of temperature, the equivalent stresses and surface velocities have been compared for the steady state flow conditions.

The equivalent stress in Figure 4-4 is shown as a function of time for various flow laws (Glen, Hooke, Nye) for Element 12 of the twelve element mesh. It is clear that the ice mass reaches the steady state flow condition very quickly, regardless of the flow law. The two isothermal ice masses (Nye, Hooke) shown for comparison to the non-isothermal ice mass using Glen's law indicate that Glen's law (at 0°C) and Nye's law (at -0.08°C) give almost identical results. Increasing the temperature non-uniformity tends to increase the steady state stress levels as the ice mass becomes colder.

Along similar lines, the equivalent stresses for Elements 11 and 43 of the 48 element mesh (Figure 3-3 in Chapter 3) are given in Table 4-1 for various temperature distributions and functional flow relationships H_{BTW} . The steady state surface velocity for the ice mass based on this law are given in Table 4-2, and are also shown schematically in Figure 4-3. Once again, the influence of temperature is significant.

Surface velocities (velocity distribution) for the Barnes

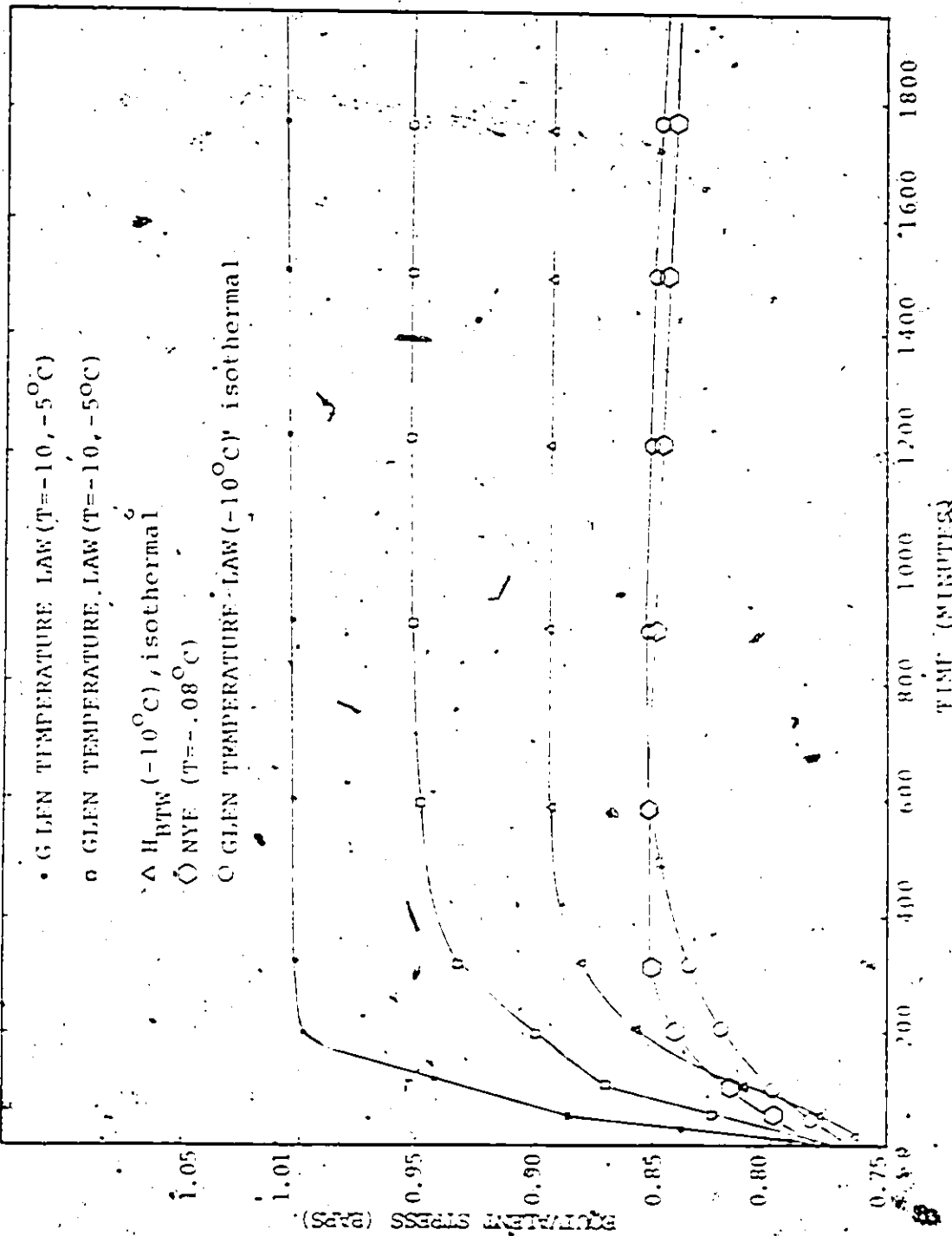


FIGURE 4-4 EQUIVALENT STRESS - ELEMENT 12 OF TWENTY ELEMENT MESH (FIGURE 4-2)

TABLE 4-1 EQUIVALENT STRESSES AS FUNCTION OF TIME

Time (min)	ELEMENT 11			ELEMENT 43		
	CASE A	CASE B	CASE C	CASE A	CASE B	CASE C
200	0.217	0.206	0.245	0.329	0.265	0.493
300	0.214	0.216	0.201	0.330	0.235	0.410
600	0.205	0.232		0.339	0.251	
1000	0.200	0.233	0.191	0.345	0.248	0.400
1500	0.196	0.233	0.180	0.347	0.246	0.413
2000	0.195	0.234	0.176	0.344	0.242	0.420
3000	0.198	0.235	0.169	0.346	0.235	0.432
4000	0.201	0.237	0.162	0.327	0.228	0.446
5000	0.205	0.239	0.160	0.319	0.221	0.451
10000	0.223	0.249	0.157	0.296	0.203	0.456

*See Figure 4-3 for Case, 48 element mesh

TABLE 4-2 STEADY STATE SURFACE VELOCITIES (m/a)

SURFACE NODE NO case	5		10		15		20		25		29		32		34	
	V _x	V _y	V _x	V _y	V _x	V _y	V _x	V _y	V _x	V _y	V _x	V _y	V _x	V _y	V _x	V _y
a	0.0	-0.468	0.429	-0.396	0.909	-0.339	1.331	-0.304	1.655	-0.309	1.835	-0.292	1.200	-0.275	0.774	-0.161
c	0.0	-0.125	0.105	-0.107	0.227	-0.089	0.344	-0.074	0.432	-0.699	0.461	-0.064	0.279	-0.269	0.182	-0.038
b	0.0	-0.330	0.245	-0.193	0.503	-0.177	0.700	-0.173	0.868	-0.191	0.993	-0.186	0.707	-0.162	0.449	-0.094

Ice Cap, based on field measurements and steady state results from the finite element analyses, are shown in Figure 4-5 a and b. The various velocities obtained when the best available flow relationships (including functional forms developed here) and temperature distribution for the Barnes Ice Cap were adopted are compared in Figure 4-5. It appears that the steady state surface velocity distributions from the finite element analysis do not compare favourably with the velocity distribution based on observed results for any flow relationship. However, surface velocities from field measurements are based on average yearly movements while many glaciers advance more rapidly in the summer than they do in the winter. Of course for large ice masses, this will be mainly a surface feature as the bulk of the ice does not change in temperature with season. Thus, observed velocity distributions must be treated with caution since they may reflect average yearly values, not true velocities for any given time of the year. On the other hand, because flow relationship data used in the current finite element model of the Barnes Ice Cap are derived from Hooke's measurements made during the summer very near to the southern margin, the simulation model probably reflects these more rapid summer results (15). It is possible that the simulation model is actually yielding reasonable surface velocities, and that the averaged yearly results and use of specific flow relationship data from near the margin of the

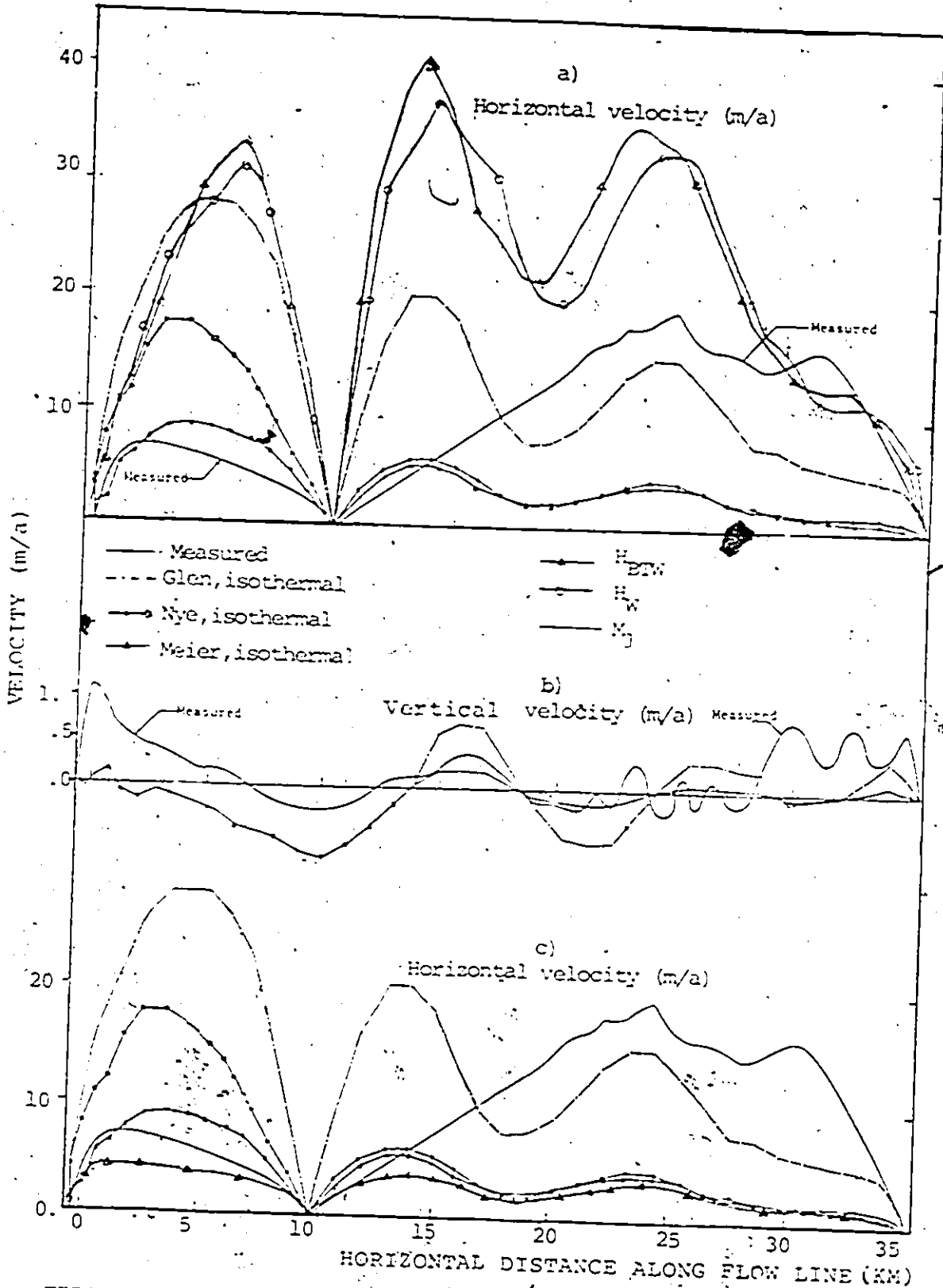


FIGURE 4-5 COMPARISON OF STEADY STATE SURFACE FLOW RATES, BARNES ICE CAP

Barnes Ice Cap are observing the actual ice mass field conditions.

To examine the possible consequences of using averaged yearly surface velocities, Table 4-3 was developed to show hypothetical summer surface velocities compared to average yearly values. If the Barnes Ice Cap southern margin behaves as an ice mass whose summer is typically four months long, over which 50% of the yearly surface deformation occurs in the summer, then it can be seen from Table 4-3 that the summer surface velocity is 150% of the averaged yearly surface velocity. If the observed results were then corrected to account for these hypothetical summer surface velocities, comparisons with the finite element method results will then show much closer agreement between predicted and observed results if the functional form flow laws H_{BTW} or H_w are used (base laws derived from Barnes Ice Cap data). While this discussion is based on a hypothetical consideration of summer surface velocities, this aspect of the simulation should certainly be extended in future studies.

The results discussed above clearly indicate that the in situ temperature distribution has a significant influence on the flow behaviour of ice masses. Comparing observed annual surface velocities of the Barnes Ice Cap to steady state finite element method simulation results, it was found that the agreement was generally poor for all flow laws considered.

TABLE 4-3

HYPOTHETICAL SURFER SURFACE VELOCITIES*

Length of Surfer (months)	Δ_s Surfer Velocity as Percent of Average	Δ_s / Δ_T Percent Movement
2	180	30
2	240	40
2	300	50
2	360	60
2	420	70
3	120	30
3	160	40
3	200	50
3	240	60
3	280	70
4	90	30
4	120	40
4	150	50
4	180	60
4	210	70
5	72	30
5	96	40
5	120	50
5	144	60
5	168	70

Explanation of Table 4-3

In general:

$$V = \Delta_T / t$$

where V is the velocity, Δ_T is the movement in the time interval t. Now:

$$\Delta_T = \Delta_s + \Delta_w$$

where s and w refer to summer and winter. If the surfer displacement

$$\Delta_s = .6\Delta_T$$

and t is four months, or:

$$V_s = (.6/4)\Delta_T$$

The average velocity (yearly) is $\Delta_s / 12$ and therefore the ratio of surfer to yearly velocity is 1.8. The surfer velocity can be written

$$V_s = 1.8V_{\text{average}}$$

However, the observed surface velocities are the annual average rates which may be considerably less than the summer rates near the margin. The steady state finite element method simulation results for functional flow laws H_{BTW} and H_w based on data from the Barnes Ice Cap Margin, may prove to be more reasonable if this effect is considered in developing flow relationships appropriate for the total ice mass.

4-5

THERMAL PROPERTIES OF ICE AND ICE MASSES

Future finite element simulation will consider both the transient heat flow characteristics and creep behaviour of ice masses. Since this will require a knowledge of the thermal properties of ice, as well as the strength properties involved, this section will deal briefly with the thermal properties involved. The general transient heat transfer equation applicable for a glacier, which must be solved in the coupled problem is:

$$\frac{\partial}{\partial x} (K_x \frac{\partial t}{\partial x}) + \frac{\partial}{\partial y} (K_y \frac{\partial t}{\partial y}) + \frac{\partial}{\partial z} (K_z \frac{\partial t}{\partial z}) + \dot{Q} - C_p \frac{\partial t}{\partial t} = 0 \quad (4-1)$$

where t is the temperature, K_x , K_y , and K_z are the thermal conductivities in the x , y , and z directions, \dot{Q} is the heat flow (friction, radiation, rain), and C_p is the specific heat. In addition, the surface temperatures must be known and on the surface:

$$K_x \frac{\partial t}{\partial x} i_x + K_y \frac{\partial t}{\partial y} i_y + K_z \frac{\partial t}{\partial z} i_z + \dot{Q}_s + \alpha(t_f - t_s) \quad (4-2)$$

where \bar{q} is boundary heat input, i_x , i_y , i_z , are direction cosines in the x, y, and z directions, and α is the film coefficient. A program for the above thermal analysis has recently been developed by Mirza (73) and will be used during an extension of the current study. Factors to be considered include: albedo, thermal conductivity, rainfall, radiation, geothermal flux, wind, and friction.

Albedo

Ice surfaces normally reflect about 60% of the incoming radiation, although covering the surface with dirt can reduce this to 20%. Paterson suggests that the albedo of snow varies as it ages from 70-90% reflection when fresh, to only 20-40% when it becomes ice (7).

Thermal Conductivity

The thermal conductivity of ice has been determined by various researchers who have found that for the temperature range of most ice masses that K varies inversely with temperature, somewhat with crystal orientation, but does not vary with crystal size or source of the ice (18). Typical relationships for thermal conductivity which are available are given in Table 4-4.

External Heat Sources

There are several well-recognized sources of external heat including rain, geothermal flux, radiation, and friction to be considered.

TABLE 4-4
THERMAL CONDUCTIVITY OF ICE

Researcher	Thermal Conductivity	Comment
Dillard, Timmerhaus (78)	$K = 2.715 - 3.403 \times 10^{-3} T_C + 9.085 \times 10^{-5} T_C^2$	$T = 0$ to -165°C
Dillard, Timmerhaus (78)	$K = 488.19/T_K + 0.4685$	$T = 0$ to -165°C in Watt/m-deg
James (79)	$K = \rho C_p (8.43 - 0.101 T_C) \times 10^{-3}$	$T = 0$ to -40°C
Mellor (80)	$K = 0.0085 T_C^2$	for snow in cal/cm-sec- $^\circ\text{K}$

1. Rainfall

Rainfall contributes heat equal to the heat of the volume of water that precipitates and this heat is given by:

$$Q_r = C_w p (t_{\text{rain}}^{\circ} - t_c^{\circ}) \quad (4-3)$$

where C_w is 80 cal/cm³, and p is the rate of precipitation. This contribution is generally small due to the nature of the climate in glacial regions (7).

2. Radiation

Radiation from the sun, thought to be the main contributor to the energy of ice masses, is proportional to the angle of incidence of the radiation. Monthly radiation values of less than 10 langelies (1 langely = 1 gram cal/cm²) to several hundred langelies per month are appropriate for Baffin Island (Barnes Ice Cap) depending on the season (74, 76). To model the Barnes Ice Cap, either monthly or daily records could be used to determine the quantity of incoming radiation. Such records are found in the Canadian Monthly Record (76).

Geothermal Flux

Dissipation of the earth's primal heat (77) causes heat flow through the earth's crust into the glacier as an external heat source at the glacier base (about 1.2 kcal/cm²-sec (37)). Typical values of geothermal flux in Northern Canada are given in Table 4-5.

Table 4-5

TYPICAL GEOTHERMAL FLUX @ NORTHERN CANADA

Researcher	Location	Year	Geothermal Flux mW/m ² *
Jessop, Hobart, Slater (80)	Kirkland Lake	1951	42
Jessop, Hobart, Slater (80)	Resolute Bay	1955	121
Jessop, Hobart, Slater (80)	Norman Wells	1962	83
Smith (81)	Average (N.W.T.)	1969	41
Smith (81)	Interior Lowlands	1969	62.5
Smith (81)	Canadian Shield	1969	42

* 1 W/m² = 0.0418 kcal sec⁻¹, 1 mW = .001 W

7

Wind

Convection currents carry heat to and from the glacier surface. To determine the amount of heat involved the film coefficient must be known. This film coefficient is defined by:

$$h = -K \frac{\partial T}{\partial n} / (t_s - t_f) \quad 4-4$$

where K is the conductivity, $\frac{\partial T}{\partial n}$ is the variation of temperature normal to the surface, and t_s and t_f are the fluid and surface temperatures respectively. The turbulent heat supply is then:

$$Q_w = \rho (t_f - t_s) = C_p \rho K_H \frac{\partial T}{\partial n} \quad 4-5$$

where Q_w is the heat supply, C_p is the specific heat, ρ is the fluid density and K_H the Eddy diffusivity (7, 8, 9). The value of K_H (Paterson's A_H) is approximately:

$$.16 u z \log(z/z_0) \quad 4-6$$

where u is the velocity, z is the height above the surface, and z_0 the roughness term (7, 8). In any temperature distribution analysis, a realistic radiation and wind history could be obtained from Environment Canada Reports (ICE, 74).

Friction

While not discussed here, friction should be considered in the heat flow analysis of ice masses. The work of Weertman, Liboutry, and Budd (10, 54, 55) provides detailed information

on the incorporation of friction and its quantification.

Coefficient of Expansion

When a coupled (or decoupled in an incremental solution) heat flow - creep finite element method simulation model is considered, the coefficient of thermal expansion (α_e) must be known. α_e is independent of crystal orientation, although it decreases with temperature. Typical values of α_e are given in Table 4-6.

4-6

SUMMARY

In this Chapter, the influence of temperature distribution on ice flow was shown to be important enough to significantly effect the anticipated flow behaviour of a large ice mass such as the Barnes Ice Cap. Further, it was found that ice flow rates predicted by a cold non-isothermal simulation model of the Barnes Ice Cap lead to surface velocities which do not in general compare favourably with observed results. Finally, the thermal properties of ice and ice masses needed for a coupled heat flow-creep analysis were summarized.

TABLE 4-6
COEFFICIENT OF THERMAL EXPANSION (α_e) (18)

Temperature °C	α_e (10^{-6} deg^{-1})
0	52
-50	42
-100	32

CHAPTER 5

SUMMARY, CONCLUSIONS, AND FUTURE WORK

Glaciers are large ice masses, and in total cover ten percent of the world's land surface. With the advent of the finite element method it is possible to construct models of any of these ice masses to describe flow characteristics and temperature distribution. In this study, the behaviour of a typical cold glacier of the Canadian North, the Barnes Ice Cap, was simulated using the incremental initial strain finite element method. Several important aspects relevant to the numerical modelling of ice masses were studied, including:

1. functional flow laws
2. initial stress conditions (in situ stress state)
3. temperature distribution.

A functional flow law is an important and necessary materials description needed in the finite element method simulation since each material has its own flow characteristics. Since flow laws are generally power functions of the stress, a small error can be greatly magnified. A survey of the available work done with regard to empirically determined flow laws and the conditions under which the laws were derived was carried out. Further, the movement of dislocations in a crystal lattice, and parameters which are

important to the movement of dislocations through the lattice were briefly considered. It was found that in deriving a flow law for ice that empirical work has not controlled with sufficient attention those parameters which a consideration of the movement of dislocations shows to be very important. Several functional flow laws were proposed to deal with the simulation of the non-isothermal Barnes Ice Cap. These laws, designated H_{BTW} , H_W , M_1 , and M_2 , were derived from base laws which originally did not consider the temperature variation of flow rate, but were extended by assuming the creep deformation of ice to be thermally activated.

The influence of initial stress states on glacier flow has been examined. Glaciers may have a "memory" of previous stress states imposed on the elastic state of stress under gravity. Because the finite element method simulation of glaciers has in the past considered only the possibility of stress states due to gravity, it was necessary to determine the importance of other than this stress state. It was found that the "memory" of past stress states is important to glacier flow. The differences between observed flow rates and finite element method predictions of the flow rates of glaciers may be in part due to the lack of knowledge of the in situ stress state. It may be necessary to determine

the state of stress in a glacier based on observations of surface flow rates, rather than assuming the gravity state of stress prevails.

The creep rate of ice for a temperature variation of as little as 5°C changes almost be an order of magnitude. The importance of non-isothermal conditions on the behaviour of ice masses was investigated. It was found that the flow of ice masses is significantly influenced by temperature distribution. The in situ temperature distribution of ice masses must be known. Using the temperature distribution based on observed field results and a simple mathematical model, and using the functional flow laws proposed in this study, the Barnes Ice Cap was modelled using the finite element method. It was found that the non-isothermal Barnes Ice Cap steady state finite element surface velocities predicted did not compare favourably with the observed flow rates. This may be because the methods used to derive or reduce data yield average values. However, factors such as stress states and ice characteristics must be considered in more detail before improved results are obtained.

Two finite element approaches have been used to solve creep problems: the explicit scheme which determines the solution at any increment as a function of the previous; and the implicit scheme which determines the solution at any increment as a function of the present and previous

increment. It was found that the steady state solution predicted by both schemes was the same, but that the implicit scheme was more efficient.

Future research must:

- 1) consider systematically the parameters influencing the creep of ice;
- 2) consider the initial stress conditions;
- 3) incorporate large deflection theory into the finite element method to model glacier surging; and
- 4) couple temperature distribution with the flow of ice masses.

REFERENCES

1. Desai, Abel, Introduction to the Finite Element Method, Van Nostrand Reinhold, 1976.
2. Emery, J.J., "Finite Element Analysis of Creep Problems in Soil Mechanics", Ph.D. Thesis, University of British Columbia, 1971.
3. Greenbaum, G.A., "Creep Analysis of Axi-Symmetric Bodies", Ph.D. Thesis, University of California, Los Angeles, 1966.
4. Nguyen, T.Q., "Simulation of Ice Flow Using the Finite Element Method", M. Eng. Thesis, McMaster University, 1976.
5. Hanafy, E., Directed Studies, McMaster University, 1977.
6. Brown, C.B., and Evans, R.J., "Effect of Glide and Creep on Rigid Obstacles", IASH, Pub. 114, 1974.
7. Paterson, W.S.B., The Physics of Glaciers, Pergamon Press, London, 1972.
8. Raymond, C., "The Inversion of Flow Measurements for Stress and Rheological Parameters in a Valley Glacier", J. Glaciology, Vol. 12, No. 64, 1973.
9. Embleton, C., and King, A.M., Glacial Geomorphology, Second Edition, Edward Arnold, Great Britain, 1977.
10. Weertman, J., "Sliding of Non Temperate Glaciers", CRREL, 216, 1966.
11. Goldwaithe, R., "Jerky Glacier Motion and Melt Water", IASH, Pub. 95, 1973.
12. Meier, M., "Mode of Flow of Saskatchewan Glacier, Alberta, Canada", Geological Survey, Prof. Paper 351, 1960.
13. Nye, J.F., "Glacier Flow in Channels of Various Cross Sections", J. of Glaciology, Vol. 5, No. 41, 1965.
14. Mercer, J., American Geographical Society, June 1958.

15. Hooke, R.L., "Structure and Flow in the Margin of Barnes Ice Cap, Baffin Island, N.W.T., Canada", J. Glaciology, Vol. 12, No. 66, 1973.
16. Holdsworth, G., "Deformation and Flow of Barnes Ice Cap, Baffin Island", Environment Canada, No. 52.
17. Budd, Jenssen, Radok, "Derived Physical Characteristics of the Antarctic Ice Sheet", Meteorology Department, University of Melbourne, 1971.
18. Hobbs, P., Ice Physics, Oxford Press, Oxford, 1976.
19. Fletcher, Chemical Physics of Ice, Cambridge Monographs on Physics, 1970.
20. Landauer, J.K., "On the Deformation of Excavations in the Greenland Neve", SIPRE, Report 30, 1957.
21. Wakahama, G., and Narita, H., "Metamorphism from Snow to Firn and Ice in a Small Patch on Mt. Daisetu, Hokkaido, Japan", IASH, Pub. 104, 1971.
22. Mellor, M., and Smith, J.H., "Creep of Snow and Ice", CRREL, Report 220, 1966.
23. Jones, S.F., and Glen, J.W., "Mechanical Properties of Single Crystals of Ice at Low Temperatures", Bern, IASH, Pub. 79, 1967.
24. Zienkiewicz, O., The Finite Element Method in Engineering Science, McGraw-Hill, New York, 1971.
25. Ives, P., Mechanical Metallurgy 3P3, McMaster University, 1976.
26. Hobbs, B., Means, W.D., and Williams, P.P., An Outline of Structural Geology, John Wiley & Sons, Toronto, 1976.
27. Ashby, M.F., and Frost, D.J., Seven Case Studies in the Use of Deformation Maps and the Construction of Transient Maps and Structure Maps, Cambridge University, 1976.
28. Ashby, M.F., and Frost, D.J., "Deformation Mechanism Maps Applied to the Creep of Elements and Simple Inorganic Compounds", in Frontiers in Materials Science, editors Muir and Stein, Marcel Dekker Inc., New York, 1976.

29. Burton, B., "Diffusional Creep of Polycrystalline Materials", Diffusion and Defect Monograph Series, Trans-Tech Publications, 1977.
30. Coldbeck, S.J., "Isua, Greenland: Calculations of Glacier Flow for Open Pit Mine", CRREL, Report 309, 1973.
31. Johnston, W., and Mellor, P.J., Engineering Plasticity, Van Nostrand Reinhold, 1973.
32. Mendelson, A., Plasticity: Theory and Application, MacMillan, New York, 1968.
33. Nye, J.F., "Flow Law of Ice from Measurements in Glacier Tunnels; Laboratory Experiments, and the Jungfraufirn Borehole Experiment", Proc. Roy. Soc., Series A, Vol. 219, No. 1139, 1951.
34. Kuo, S., "Stress and Time Effect on the Creep Rate of Polycrystalline Ice", Ph.D. Thesis, Michigan State University, 1972.
35. Glen, J.W., "Creep of Polycrystalline Ice", Proc. Roy. Soc., Series A., Vol. 228, 1955.
36. Steinman, S., "Résultats Expérimentaux sur la Dynamic de la Glace et leur Corrélation avec le Mouvement et la Pétrographie", IASH, Pub. 47, 1958.
37. Nakaya, U., "Viscoelastic Properties of Snow and Ice in Greenland Ice Cap and Bending of Single Crystals", Chamonieux, IASH, Pub. 47, 1958.
38. Krausz, A.S., and Eyring, H., Deformation Kinetics, John Wiley, 1975.
39. Krausz, A.S., "The Creep of Ice in Bending", Canadian J. of Physics, Vol. 41, No. 1, 1963.
40. Krausz, A.S., "The Activation Volume Associated with the Plastic Deformation of Ice", NRCC, 12806, 1972.
41. Butkovich, T.R., and Landauer, J.K., "The Flow Law for Ice", Chamonieux, IASH, Pub. 47, 1958.
42. Barnes, P., Tabor, D., Walker, J.C.F., "The Friction and Creep of Polycrystalline Ice", Proc. Roy. Soc. London, Series A, No. 324, 1971.

43. Paterson, W., "Temperature Measurements in Athabaska Glacier, Alberta, Canada", J. Glaciology, Vol. 10, 1971.
44. Landauer, J.K., "Some Preliminary Observations on the Plasticity of Greenland Glaciers", SIPRE, Report 33, 1957.
45. Miller, M., "Phenomena Associated with Deformation of a Glacier Borehole", Toronto, IASH, Pub. 46, 1957.
46. Robin, G., "Stability of Ice Sheets as Deduced from Deep Temperature Gradients", Hanover, IASH, Pub. 86, 1968.
47. Classen, D., "Temperature Profile For Barnes Ice Cap Surge Zone", J. Glaciology, Vol. 18, No. 80, 1977.
48. Holdsworth, G., and Bull, C., "The Flow Laws of Cold Ice Investigations on Meserve Glacier, Antarctica", Hanover, IASH, Pub. 86, U.S.A., 1969.
49. Matthews, W.H., "Velocity Distribution, Salmon Glacier", J. Glaciology, Vol. 3, 1958.
50. Weertman, J., "Creep of Ice", Physics and Chemistry of Ice, Roy. Soc. Canada, Ottawa, 1972.
51. Butkovich, T.R., and Landauer, J.K., "Creep of Ice at Low Stresses", SIPRE, Report 72, 1960.
52. Hansen, B.L., and Landauer, J.K., "Some Results of Ice Cap Drill Hole Measurements", Chamonieux, IASH, Pub. 47, 1958.
53. Nye, J.F., Proc. Roy. Soc., A207, 1951.
54. Budd, W.F., "Dynamics of Ice Masses", ANARE, 1969.
55. Higasaki, A., "Mechanical Properties of Single Ice Crystals", in Physics of Ice, Plenum Press, New York, 1969.
56. Shumskii, P.A., "On the Theory of Glacier Motion", Helsinki, IASH, Pub. 55, 1960.
57. Bromer, D.J., and Kingery, W.D., "Flow of Polycrystalline Ice at Low Stresses and Small Strains", J. Applied Physics, Vol. 39, No. 3, 1968.
58. Jellef, H.H.G., and Brill, R., "Viscoelastic Properties of Ice", J. Applied Physics, Vol. 27, No.10, October, 1956.

59. Vialov, S.S., "Regularities of Ice Deformation", Chamonieux, IASH, Pub. 47, 1958.
60. Rigsby, G., "Fabric of Glacier and Laboratory Deformed Ice", IASH, 1963.
61. Gold, L.W., "Initial Creep of Columnar Grained Ice", NRC 8475, Ottawa, Aug., 1965.
62. Goodman, D.J., Frost, H.J., and Ashby, M.F., "The Effect of Impurities on the Creep of Ice and its Illustration by the Construction of Deformation Maps", IASH, 1977.
63. Dantl, G., "Elastic Moduli of Ice", in Physics of Ice, Plenum Press, New York, 1969.
64. Craig, R.F., Soil Mechanics, Van Nostrand Reinhold, Scarborough, 1975.
65. Hanafy, E., Finite Element Simulation of Tunnel Excavations in Creeping Rock, M. Eng. Thesis, McMaster University, March, 1976.
66. Mirza, F., "Large Deflection and Creep (Implicit Formulation), Calculation of F_{nD} and F_{nC} ", Internal Report, Department of Civil Engineering, McMaster University, 1978.
67. Milne, W.E., Numerical Solution of Differential Equations, Dover Publications Inc., New York, N.Y., 1970.
68. Pinder, Gray, "Finite Element Simulation in Surface and Subsurface Hydrology", Academic Press, 1977.
69. Mirza, F., "Geometrically Nonlinear Problems", Internal Report, Department of Civil Engineering, McMaster University, 1978.
70. Post, A., "The Recent Surge of Walsh Glacier, Yukon and Alaska", J. of Glaciology, Vol. 3, No. 3, 1966.
71. Boulton, G.S., Jones, A., "Flow of Ice Over Deformable Beds", Dynamics of Large Ice Masses, Ottawa, 1978.
72. Holdsworth, G., Temperature Profile of Barnes Ice Cap Based on Robins Steady State Model, Communication to J.J. Emery, 1977.
73. Mirza, F., "Heat Analysis Program Written While at McMaster University", 1978.

74. -----Environment Canada, Ice Summary and Analysis, 1971, 1972.
75. Raymond, et al., "Calculations of Velocity and Temperature in Polar Ice Masses Using the Finite Element Method", Dynamics of Large Ice Masses, Ottawa, 1978.
76. -----, Canadian Monthly Record, Environment Canada.
77. Stacey, F.D., Physics of the Earth, Second Edition, Wiley, New York, 1977.
78. Dillard, D.S., Timmerhaus, K.D., "Low Temperature Thermal Conductivity of Solidified H₂O and D₂O", Pure Appl. Cryogen, Vol. 4.
79. James, G., "The Thermal Diffusivity of Ice and Water Between -40° and +60°C", Journal of Material Science, Vol. 1, No. 3, 1968.
80. Mellor, M., "Polar Snow - A Summary of Engineering Properties", in Ice and Snow, MIT Press, 1963.
81. Jessop, A.M., Hobart, M.A., Slater, J.G., "The World Heat Flow Data Collection 1975", EM and R, Geothermal Series, No. 5, 1976.
82. Smith, P.J., Topics in Geophysics, MIT Press, 1973.
83. Kraus, H., "An Energy Balance Model for Ablation in Mountainous Areas", Moscow, IASH, Pub. 104, 1978.
84. Derikx, L., "The Heat Balance and Associated Runoff from an Experimental Site on a Glacier Tongue", Moscow, IASH, Pub. 104, 1975.
85. Lliboutry, L., "Théorie Complète du Glissement des Glaciers, Compte Tenue du Fluage Transitoire", Bern, IASH, Pub. 79, 1968.
86. Poirier, J.P., Plasticité à Haute Température des Solides Crystalline, Eyrolles, 1976.
87. Weertman, J., "Theory of Steady State Creep Based on Dislocation Climb", J. Applied Physics, Vol. 26, 1955.
88. Mukherjee, A.K., Bird, J.E., Dorn, J.E., "Experimental Correlations for High Temperature Creep", ASM, Vol. 62, 1969.

APPENDIX 1
SHEAR STRESS

Many simple relationships have been derived in the past to deal with limiting cases of complex problems. This Appendix is included to demonstrate the derivation for a shear stress relationship frequently used in glaciology, and the limitations to which its application must be subject.

Assume that the glacier shown in Figure A1-1a is under a state of gravity stress. The average basal shear is to be found over the section shown between a_1 and a_2 . The section of interest is idealized as shown in Figure A1-1b to allow simplification of the treatment.

From Figure A1-1b, the depths h_1 , and h_2 , and the rate of change of depth are:

$$\begin{aligned} h_1 &= \{L + (X_2 - X_1)\} \sin (\alpha_s - \alpha_b) \\ h_2 &= L \sin (\alpha_s - \alpha_b) \end{aligned} \quad \text{(A1-1)}$$

and

$$\frac{h_1 - h_2}{X_1 - X_2} = -\sin (\alpha_s - \alpha_b)$$

where α_s and α_b are the ice surface and basal slopes, respectively.

To determine the shear stress the ice mass must be in a state of equilibrium. The various forces are:

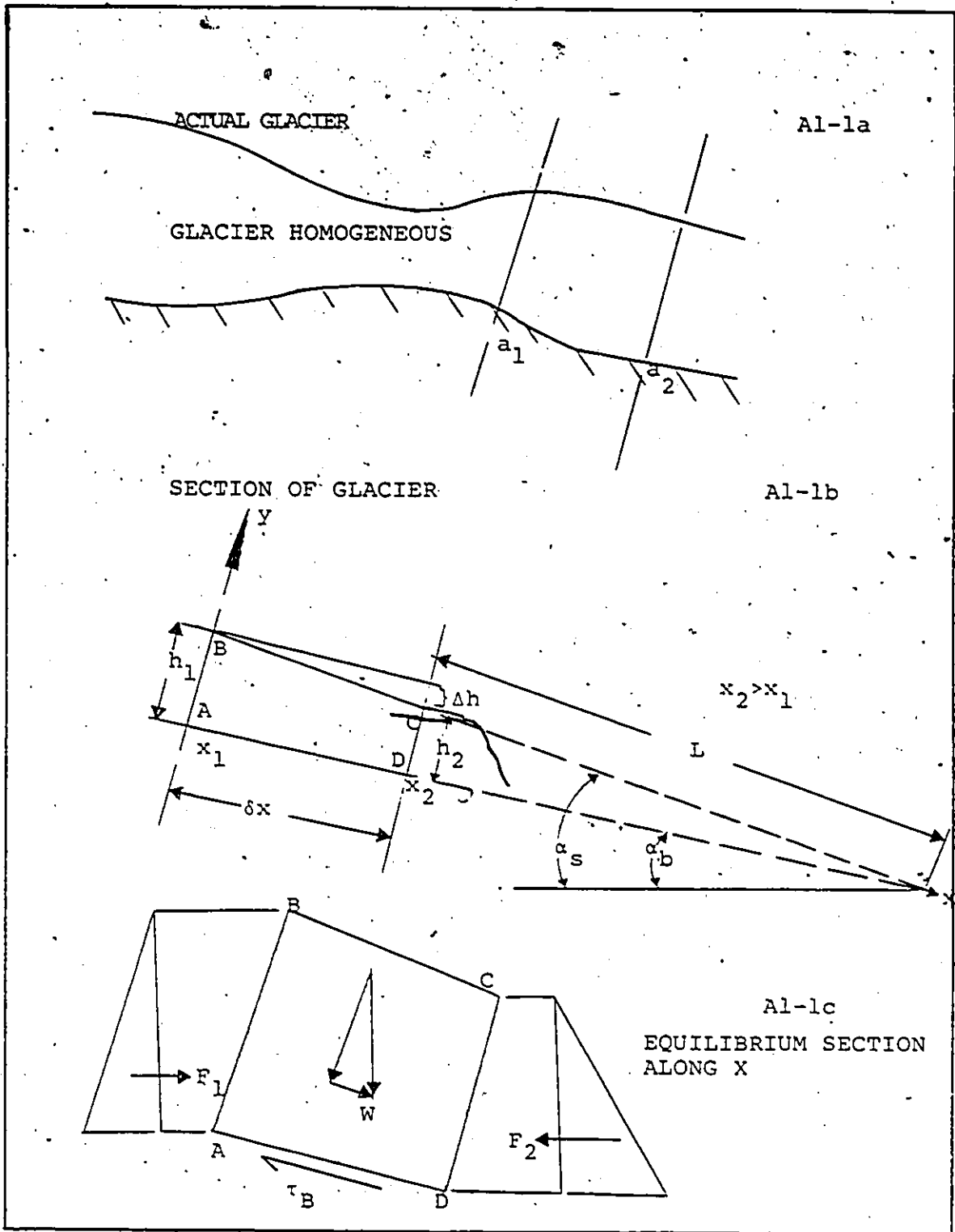


FIGURE A1-1 GLACIER SECTIONS

$$F_1, \text{ the force on AB} = \frac{1}{2} \gamma h_1 \cos^2 \alpha_b \quad (A1-2)$$

$$F_2, \text{ the force on CD} = \frac{1}{2} \gamma (h_1^2 + 2h_1 \frac{dh}{dx} \delta x + (\frac{dh}{dx} \delta x)^2) \cos^2 \alpha_b \quad (A1-3)$$

$$W, \text{ the weight component of ABCD along } x \text{ is} \\ = \frac{\gamma}{2} (2h_1 + \frac{dh}{dx} \delta x) \delta x \sin \alpha_b \quad (A1-4)$$

$$T, \text{ the shear force is } \tau_b \delta x, \quad (A1-5)$$

Force equilibrium along x implies the sum of F_x is zero, ($\Sigma F_x = 0$):

$$\Sigma F_x = 0 = F_1 - F_2 - W + T \\ = \left\{ \frac{1}{2} \gamma h_1^2 - \frac{1}{2} \gamma (h_1^2 + 2h_1 \frac{dh}{dx} \delta x + (\frac{dh}{dx} \delta x)^2) + \frac{\gamma}{2} (2h_1 + \frac{dh}{dx} \delta x) \delta x \sin \alpha_b + \tau_b \delta x \right\} \cos^2 \alpha_b \\ = 0 \quad (A1-6)$$

Now, if \cos^2 is almost unity ($\alpha_b = 0$), then

$$\tau_b = -\gamma h_1 \frac{dh}{dx} - \frac{\gamma}{2} (\frac{dh}{dx})^2 \delta x^2 + \gamma h_1 \sin \alpha_b + \frac{dh}{dx} \delta x \sin \alpha_b \quad (A1-7)$$

Assuming that all terms containing $(\frac{dh}{dx})^2$ and $\frac{dh}{dx} \sin \alpha_b$ are small, then:

$$\tau_b = -\gamma h_1 \frac{dh}{dx} + \gamma h_1 \sin \alpha_b \quad (A1-8)$$

BUT:

$$\frac{dh}{dx} = \sin (-\alpha_s + \alpha_b) \quad (A1-9)$$

and therefore A 1-8 becomes:


$$\tau_b = -\gamma h_1 \sin (\alpha_s - \alpha_b) + \gamma h_1 \sin \alpha_b \quad (A1-10)$$

Assuming $(\alpha_s - \alpha_b)$ small and α_b small then:

$$\tau_b = \gamma h_1 \alpha_s$$

(A1-11)

Equation A1-11 is applicable in situations of small surface slope and base slope, but not for large slopes or where the surface and base slopes differ significantly.



APPENDIX 2

DISLOCATIONS, DEFECTS AND DEFORMATION

This Appendix is intended for those seeking more details concerning the micromechanistic behaviour of materials, without having to refer to outside references. Crystalline materials, ice, metals and minerals, are made of a regular repetitive arrangement of molecules, this arrangement having imperfections of various types.

Imperfections

The possible types of imperfections are:

1. Point (substantial impurity, interstitial vacancy, self interstitial, Skottky, Frenkel);
2. Line (screw or edge);
3. Interfacial (crystal boundary, stacking faults), and ;
4. Bulk (voids or inclusions).

These imperfection types are shown in Figure A2-1. The various types of defects will have different influences on the creep behaviour of polycrystalline materials, and in fact, creep deformation as a rate process is dependent on the presence of such defects.

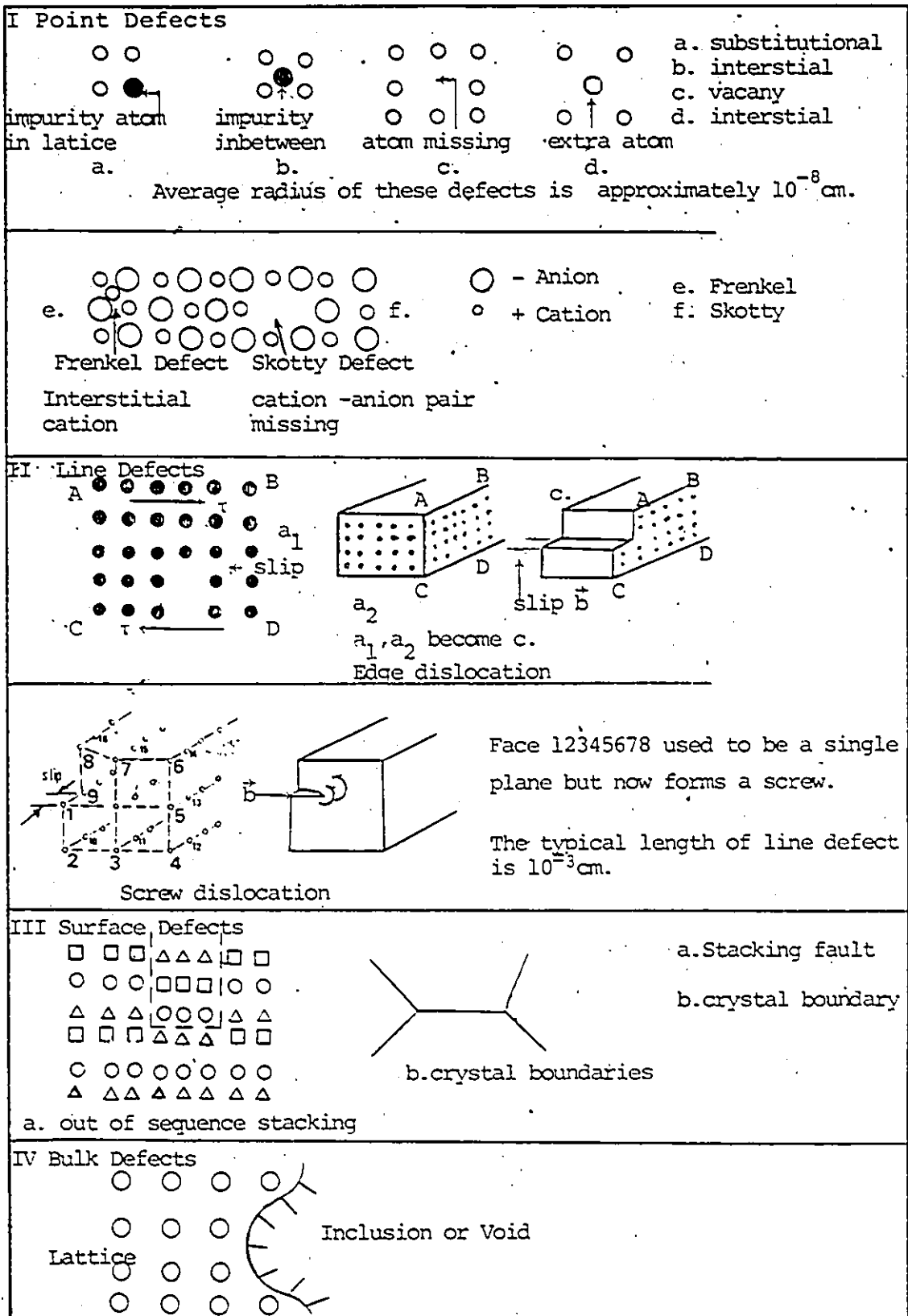


FIGURE A 2-1 TYPES OF DEFECTS

Nabbaro-Herring Creep

These defects are controlled by diffusion processes and other factors. Grain boundary or lattice diffusion creep, also called Coble or Nabbaro-Herring creep, as illustrated in Figure A2-2, is facilitated by increasing the number of line defects or grain boundary defects. In Figure A2-2, a tensile stress (i.e. shear stress at faces) is causing the flux of material from the interior of the crystal to the edges, resulting in a strain rate:

$$\dot{\epsilon} = B\sigma\Omega/d^2KT \quad (A2-1)$$

where $\dot{\epsilon}$ is the strain rate, σ is the stress, Ω is the atomic volume, D is the diffusion coefficient, d is the grain size, K is a constant, T is a temperature, and B is a constant (Table A2-1).

Assuming Fick's Law* applies, Equation A2-1 is known as the Nabbaro-Herring Creep equation, where volume diffusion values are applicable for D .

Coble Creep

When diffusion results in material moving along the grain boundary, the process is called Coble Creep and the

* Flux = $D \frac{\partial C}{\partial x}$ (diffusion coefficient x concentration gradient)

TABLE A2-1
 B OF DIFFUSION EQUATION
 BURTON (29), POIRIER (86)

B IN LATTICE CREEP		
Grain Shape	Stress	B
Sphere (diameter d)	Shear	40
	Tensile	13.3
Cylinder (L=2d)	Tensile	12.2
Long square rod d ² =area	Shear	16/√2
Cube d ³	Tensile	12
Foil d x t	Tensile	7.5
	Tensile	12.0
B IN COBLE CREEP		
Grain Shape	Stress	B
Sphere	Tensile	148
	Shear	148/3
Foil	Tensile	12

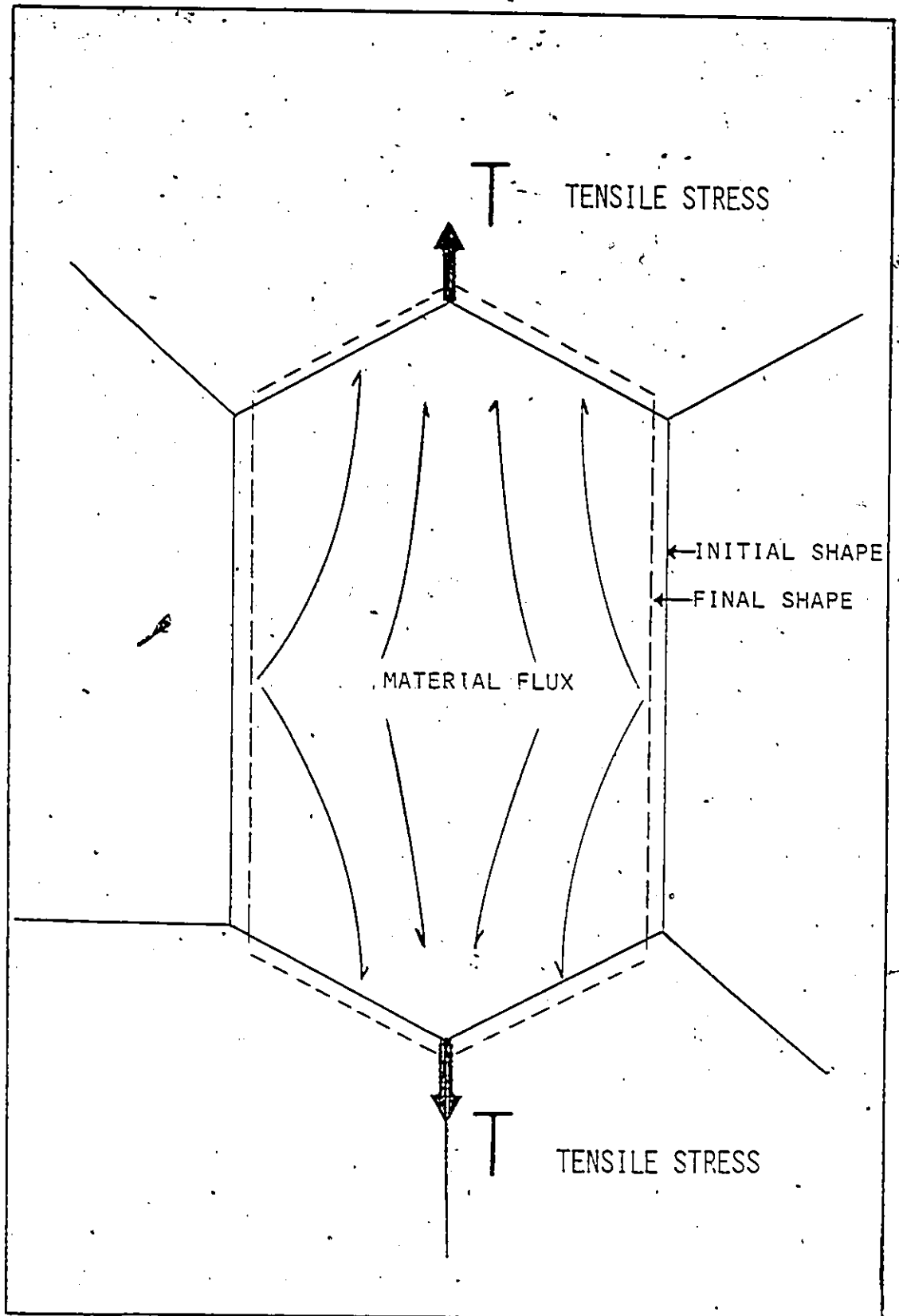


FIGURE A 2-2 CRYSTAL UNDER STRESS

resulting strain rate is given by:

$$\dot{\epsilon} = BD \delta \sigma \Omega / \pi d^3 KT \quad (A2-2)$$

where the various quantities were described earlier, but in this case edge or grain boundary values are applicable for D , and δ is the Burgers vector.

Dislocation Movements

Interstitial atoms and vacancies move by diffusion as do impurities, and may influence the creep behaviour of ice by impeding or assisting the motion of dislocations. Dislocations, known to be mobile in ice, and having typical velocities of 10^{-3} to 10^{-6} cm/sec, glide on the basal plane, and may pile up on grain boundaries to cause microcracks. Weertman and others have calculated the dislocation glide creep rate (87).

Mukerjee, Bird and Dorn (88), after reviewing many possible deformation mechanisms, found the strain rates in general could be given by:

$$\dot{\epsilon} = \frac{BDu\delta}{KT} \left(\frac{\sigma}{G}\right)^n \quad (A2-3)$$

where the various quantities were described earlier, and G is the shear modulus.

Applicability

Equation A2-3 can be used to describe many flow

relationships. When lattice and grain boundary diffusion creep occurs, Equations A2-1 and A2-2 apply. If there is grain boundary sliding on a smooth interface the strain rate becomes:

$$\dot{\epsilon} = 8\delta W_g D_T / KT \quad (A2-4)$$

where W_g is the grain boundary width (29). If the grain interface is rough, the creep rate due to sliding becomes (28):

$$\dot{\epsilon} = \lambda \tau \Omega D \left(2 + \frac{W}{L} \frac{D_G}{D} \right) / h^2 KT \quad (A2-5)$$

where λ , h , W , and L are associated with the grain boundary thickness, roughness, spacing and dimensions.

As old ice contains more dislocation, it is expected that if diffusional creep is important, then age will increase the strain rate. Similarly, surface preparation methods might lead to an increase in the number of dislocations and increase the strain rate.

When deriving the strain rate based on dislocation theory, the assumptions about average grain size, dislocation density, etc. give an insight into, for example, the reason for specimens in one test series aged for shorter or longer times behaving differently.

Theory also shows that several deformation mechanisms can act at once, the total creep being additive. Or, on the other hand, when several mechanisms are acting

but one of them slows the others down, a rate controlling process is involved. Ashby and Frost have defined regions in which both these major types of creep processes are involved, and defined regions where a certain one of them is dominant (deformation maps) (27, 28).
